April, 1992

LMSC/P009805

Final Report

NASA Contract NAS8-38106

Investigation of Solar Active Regions at High Resolution by Balloon Flights of the Solar Optical Universal Polarimeter

Definition Phase

Performing Organization

Research and Development Division
Lockheed Missiles and Space Company, Inc.

Principal Investigator

Dr. Theodore D. Tarbell
Lockheed Palo Alto Research Laboratory
Department 91-30, Building 252
3251 Hanover St.
Palo Alto, CA 94304 phone: (415)-424-4033
Email: SPAN SOLAR::TTARBELL fax (415)-424-3994

Period of Performance

July, 1989 to March, 1992

1.0 Introduction

On November 16, 1988, the Principal Investigator, Dr. Theodore D. Tarbell, received a letter from Dr. Stanley Shawhan of NASA Headquarters stating that the proposal (LMSC/D089397) for "An Investigation of Solar Active Regions at High Resolution by Balloon Flights of SOUP" was accepted for a definition phase. The nominal program was to be four years long, consisting of definition phase, confirmation for flight, test flight and long duration flight. The letter stated very clearly that the Max '91 Solar Balloon Program was highly cost constrained and that the investigation would have to be carried out for the costs proposed or be descoped or cancelled. The project was to begin January 1, 1989.

Dr. Tarbell replied to Dr. Shawhan accepting the conditions of acceptance of the balloon investigation and raising several concerns and recommendations. In particular, he urged that a data analysis phase of at least 12 months be guaranteed following each flight, that NASA move promptly to begin acquisition of the gondola and pointing system, that an informal but professional management approach be worked out between NASA and the PI so that the project could be done at low cost, and that the contracting process be started as soon as possible to begin the definition phase with minimum delay. Mr. Charles Gilbreth was chosen to be project manager and chief systems engineer for the investigation.

On January 11, 1989, Ted Tarbell visited George Nystrom of the Smithsonian Astrophysical Observatory balloon group in Cambridge, Mass. This was a very informative visit, with several hours to see the EXCITE X-Ray telescope, gondola, and pointer and to talk about accommodation of SOUP on a balloon mission with a new fine solar pointer. The SAO group was very impressive both in technical experience and reasonable engineering and management approaches to balloon experiments.

On January 19, Alan Wissinger of Perkin-Elmer visited to discuss his concept for a 3-axis fine-pointing system for SOUP, based on the existing design for the BAAMS gimbal system which P-E built in the mid-1970's.

On March 13-14, Ted Tarbell attended a Solar Physics MOWG meeting at NASA GSFC. On March 15, he visited the Balloon Project Branch at Wallops Island and briefed Harvey Needleman and David Stuchlik on the SOUP investigation and requirements for balloon hardware and operations.

On April 6, Mike Krim and Alan Wissinger of Perkin-Elmer visited Lockheed to present their new concepts for a protective cocoon-like gondola structure for SOUP. We felt the concept was original and incorporated several innovative features that were quite promising, both for needed protection and for managing convective heat flow and suppressing seeing in the vicinity of the telescope. We advised them to continue working on it and propose it to MSFC at the appropriate time.

In May, Alan Title and Ted Tarbell had a most interesting visit with Professor Vadim Karpinsky At Pulkovo Observatory in Leningrad. Karpinsky and his mentor Prof. Krat had flown 0.5 and 1.0 meter balloon solar telescopes in the late 60's and early 70's and

obtained excellent granulation data. These observations were a decade ahead of the rest of the world. We were shown movies of the balloon flight, granulation data, and the original images. It was all very impressive. Unfortunately, the government did not continue the program after the last balloon flight landed in the Volga River (the telescope and film were recovered with surprisingly little damage). More important, support for data analysis was not up to the standards of the flight program. Nevertheless, a great deal of high quality work has been done.

2.0 Definition Phase

Throughout the winter and spring, we were in frequent communication with Dave Bohlin of NASA HQ and John Davis of MSFC regarding the beginning of the definition phase of the balloon program. On April 3, we submitted a proposal for the Definition Phase ($ 200K for four months) to MSFC. On April 18, we were notified that the funding had finally been received by MSFC from Headquarters. Negotiation of the contract proceeded in fits and starts through May and early June.

On April 21, in response to requests from MSFC and NASA Headquarters, we submitted to MSFC a package of preliminary requirements for accommodating SOUP on a balloon gondola and pointing system. It consisted of brief answers to the question list received from MSFC, with references to pages in our proposal and Sunlab Instrument Interface Agreement. Referenced pages and figures were attached.

In June, Ted Tarbell received a letter dated May 24 from Lou Demas, new Program Manager for the Max '91 balloon program at NASA Headquarters. The letter announced a 2.5 year delay in our first flight, to December, 1993, and included a funding profile for planning purposes for the period 1989 to 1994. The budget profile showed very low funding for 1989 and 1990 and did not even cover modest inflation for the period of the delay, compared with the budget in our proposal. Further discussions with the managers at NASA Headquarters revealed that the budget problems might be even more serious than indicated in Demas' letter. We were advised (and we agreed) not even to begin serious definition phase planning using the dreary schedule in the letter of May 24.

In early July, we received this contract (NAS8-38106) and funding for the balloon project four-month definition phase. In the fall, the Confirmation Review was postponed and a no-cost extension granted.

The flight investigation phase of this contract was cancelled by NASA Headquarters in January, 1990, due to budgetary problems, and we were directed to devote our remaining resources to a variety of tasks. The remaining tasks, upon which Lockheed, NASA HQ and MSFC agreed, were scientific analysis and publication of data from ground-based observing with SOUP instrument components, completing the test report on low-voltage piezoelectric transducers for use in the image motion compensation system, and submission of a final report on the balloon project definition phase.

3.0 Research Phase

Before the cancellation of the flight phase, we had started testing of low-voltage PZT's at low pressures simulating those of stratospheric balloon flight. The Spacelab instrument used PZT's with voltages up to 800 V, to tilt the secondary mirror of the telescope to stabilize the image. These voltages would almost certainly cause ionization of the air and arc-over at pressures of 1–15 Torr, resulting in failure of the PZT's. Since the SOUP instrument was built, PZT's with the same performance at 100 V had become available. These were tested extensively in March and April, 1990, and no clear evidence of either corona or ionization breakdown was found at the pressures of interest. The test report is included as Appendix A.

The tunable filter and CCD camera system was shipped to La Palma in the Canary Islands in May, 1990, and set up at the Swedish Solar Observatory to observe during summer Max '91 Campaigns. This effort was supported entirely by other projects, namely OSL, SOHO, and Lockheed Independent Research. Nevertheless, the observing run provided very valuable experience in operating the ground-based version of the balloon instrument. Observing sequences made full use of the tunable filter to study activity in many lines formed from the photosphere to upper chromosphere. The run was very successful, and over 200 Exabyte tape cassettes were recorded, nearly 300 gigabytes of image data.

Dr. Ken Topka travelled to La Palma for two weeks in August, 1991, to help set up the SOUP tunable filter system at the Swedish Solar Observatory. He was the only one supported by this contract in the group of seven scientists and engineers who made the expedition. Dr. Topka observed the sun with the instrument for about 10 days and collected very high resolution data on active regions at a wide range of disk positions.

Our goal was to leave the entire instrument set up in La Palma for observing campaigns in October and December of 1991. However, in August we learned that the Orbiting Solar Laboratory mission had been postponed for many years, with zero funding for FY 1992. Since this project was the major source of support for our observing expeditions, we were not be able to observe during the fall and winter campaigns. Therefore, the remainder of work under this contract was devoted to continuing analysis of existing data from the very successful campaigns of September 1988, July 1989, summer 1990, and June 1991.

Throughout 1990 and 1991, data processing and scientific analysis of the La Palma (and previous Sacramento Peak) observations was in progress, supported by this contract as well as the other projects mentioned above. The complete bibliography of publications from this work is being submitted in the final report for the Spacelab 2 SOUP contract NAS8-32805 (which ran concurrently with this one for most of this period). One example which was largely supported by this contract is described next.

In November, a manuscript entitled "Properties of the Smallest Solar Magnetic Elements I. Facular Contrast Near Sun Center" was submitted to *The Astrophysical Journal*; it was accepted in January, 1992. The manuscript is included as Appendix B. This will be the first published account of a major study, primarily done by Dr. Topka, of the continuum

contrast of small magnetic flux tubes. He has found that the contrast varies quite rapidly with disk position, i.e., with inclination of the flux tube to the line of sight. Previously published versions of this center-to-limb variation are wrong, due to insufficient spatial resolution. The dependence on inclination angle is steep enough that variations are seen in different parts of an active region plage. Thus, there is the potential to measure inclination angles of the "weak" fields in plages, which will help establish field connectivity and may also reveal changes during evolution of an active region. In August, 1991, Dr. Topka collected very good data of this type on about a dozen active regions covering the entire range of disk position, and reduction of this data is still in progress.

Two poster papers and one talk were presented at the AGU Meeting in San Francisco, December, 1991. The talk was given by Ken Topka on "Observational Constraints on the Size of the Smallest Magnetic Features on the Sun." The posters were "Variation of Sunspot Field Geometry Inferred from Inclination Effects" (first author A. Title) and "Compressible Magneto- convection in Oblique Fields" (first author N. Hurlburt).

In January, 1992, four people from LPARL attended the Solar Research Base Enhancement Workshop (on other funds). NASA is showing renewed interest in balloon flights of optical telescopes, and Tarbell and Title contributed to the RBE report chapters on ground- and balloon-based observing. Additional work along these lines is expected to continue under a new contract.

Appendix A: PZT Test Report

ALTITUDE SIMULATION TESTS OF A LOW-VOLTAGE PZT TRANSLATOR

The proposed instrument to be used in the Investigation of Solar Active Regions at High Resolution by Balloon Flights of the Solar Optical Universal Polarimeter (SOUP) is the original SL2 SOUP Instrument, that was successfully flown on SPACELAB 2 in 1985, with selective modifications required by the differences in environment and observing platform.

The secondary mirror of the SL2 SOUP has a piezoelectrically actuated closed-loop control system using three high-voltage PZT actuators. These actuators functioned perfectly during their exposure to a near-perfect vacuum during several days on the SPACELAB 2 mission.

It is a well known fact that problems of arc-over, corona and ionization do not occur at pressures below 1 Torr. The region between 1 and 15 Torr is where arc-over and corona problems become serious when voltages above approximately 100 to 300 volts are used.

To eliminate these problems at balloon flight altitudes, it was decided that we should replace the high-voltage (1000 Volt) PZT actuators with the new low-voltage (100 Volt) units.

No information could be obtained from any source as to the behavior of the low-voltage PZT actuators in the 1 to 15 Torr region. We decided that an altitude simulation test should be performed on a specimen low voltage PZT actuator.

The most reliable source of low-voltage actuators (and one with whom Lockheed has had considerable experience over the past six years) was contacted. This is POLYTEC, a West German manufacturer of Piezoelectric products. A loan of a typical low-voltage PZT Translator was negotiated at no cost to Lockheed with an agreement to supply POLYTEC with a copy of the test results.

The actuator loaned was a POLYTEC model LVPZ 840.30 (See Figure 1) that has a nominal expansion of 45 microns at +100 Volts applied. This is a catalog stock item. Since it is not known at which voltages and pressure levels the problems, if any, of arcing, corona or ionization might occur within the PZT a test plan was formulated to subject the test translator to a series of escalating voltage and pressure tests, starting with a static bias of +50 volts and 15 Torr and ending with 125 Volt bias at 1 Torr pressure. The PZT leakage current was to be recorded along with pressure values. The test setup is sketched in Figure 2.

The plan was to soak the test unit for several 8 to 24 hour periods at the varying pressure settings from 15 to 1 Torr at a fixed bias voltage of 50 Vdc. Following this, bias voltage on the unit would be raised in 25 volt steps (up to a maximum of 125 volts) and the same pressure sequence repeated. If these tests were successful (no non-linear increases in leakage current) a 200 Hz. modulation (drive) signal of 25 volts P-P would be superimposed on a 95 Vdc bias voltage to simulate maximum dynamic operating conditions when used in the SOUP instrument operating at balloon altitudes.

The test setup was started on 3/26/90. As shown in Figure 2, physical placement of equipment was arranged to provide the shortest possible interconnecting leads between the PZT unit inside the chamber and the ORTEC preamplifier input. Additional electrostatic shielding was placed over the leads to minimize outside interference pickup. The calibration source was a 2.5 volt peak square wave (representing charge pulses of 2.5 picocoulombs) that was used to set the trigger threshold of an event/pulse counter. Any

momentary arc-over or corona effects in the PZT resulting in discharges of 2.5 or more picocoulombs could thus be recorded. Unfortunately, it turned out external interference was most, if not all, of what the event counter recorded.

First vacuum runs were made on 3/29/90 when all equipment had been assembled, calibrated and connected. A vacuum chamber in Bldg. 256 Environmental Test Lab was used throughout all tests. Several 24-hour soak periods were repeated and both static and dynamic tests were performed. Tests were completed on 4/13/90.

The test was only intermittently monitored by people. This fact accounts for varying time intervals between data entries. Test data was recorded at every voltage and/or pressure change and at both starting and ending time periods. Additional data was taken during intervening time intervals. All PZT leakage current values recorded on the data sheet are the instantaneous values at the time of recording but the current was continuously recorded on the Strip-chart recorder. Very little variation in leakage current with time was recorded and the nanoampere values recorded remained constant between any two monitored data points. The leakage current increases with voltage increases are expected as normal. Test data appears in Appendix 1.

Total time of continuous vacuum operation at pressures between 15 Torr (87,500 foot altitude) and 1 Torr (152,500 foot altitude) was 13 days and 15 hours (or 327 hours total). A careful analysis of the test data indicates that the LVPZ 840.30 POLYTEC low-voltage translator tested did not experience any significant arc-over at any time during any of the tests. Numerous extraneous pulse events were noted during the first week of the test program with very little or no effect on PZT leakage current. These were traced to coincide with local events caused by electrical appliances (elevator, door cypher lock, vacuum chamber control relays, hand tools, light switches, refrigerator, soldering irons, etc.) According to persons at Polytec, had any arc-over or corona appeared in the PZT unit, a much greater leakage current would have resulted and a lasting current increase on the order of milliamperes would have resulted. Additional shielding and grounding applied to the test setup during the second week of tests completely eliminated the extraneous pulses, consequently these early events were discounted from the data analysis.

CONCLUSIONS AND RECOMMENDATIONS: We feel that no 100% firm statement can be made about the occurrence or non-occurence of corona or ionization break-overs since the unit was not under observation at all times. However, it can be stated that no clear evidence of either corona or ionization breakover occuring could be found.

In view of the above test results it is recommended that the high voltage translators in the SOUP secondary mirror be replaced with POLYTEC's LVPZ low-voltage translators for any future observations to be carried out using the SOUP instrument at balloon flight altitudes.

As an additional note, during a vacation trip at the end of 1990 which included a visit to Polytec in Waldbronn, Germany, Mr. Nick Marshall of Lockheed learned that Polytec has now developed a new technique of PZT stack sealing and assembly that provides additional protection against possible leakage and corona during the critical 1 to 15 Torr exposure of low-voltage PZT translators. These units are currently being produced by Polytec on special order.

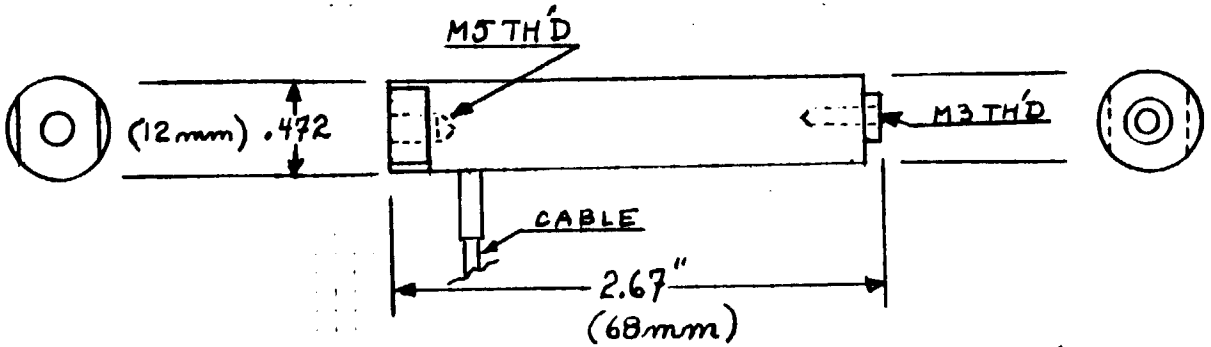

SCALE: 1:1 (ACTUAL SIZE)

POLYTEC
P-840.30 LVPZ TRANSLATOR

FIGURE 1

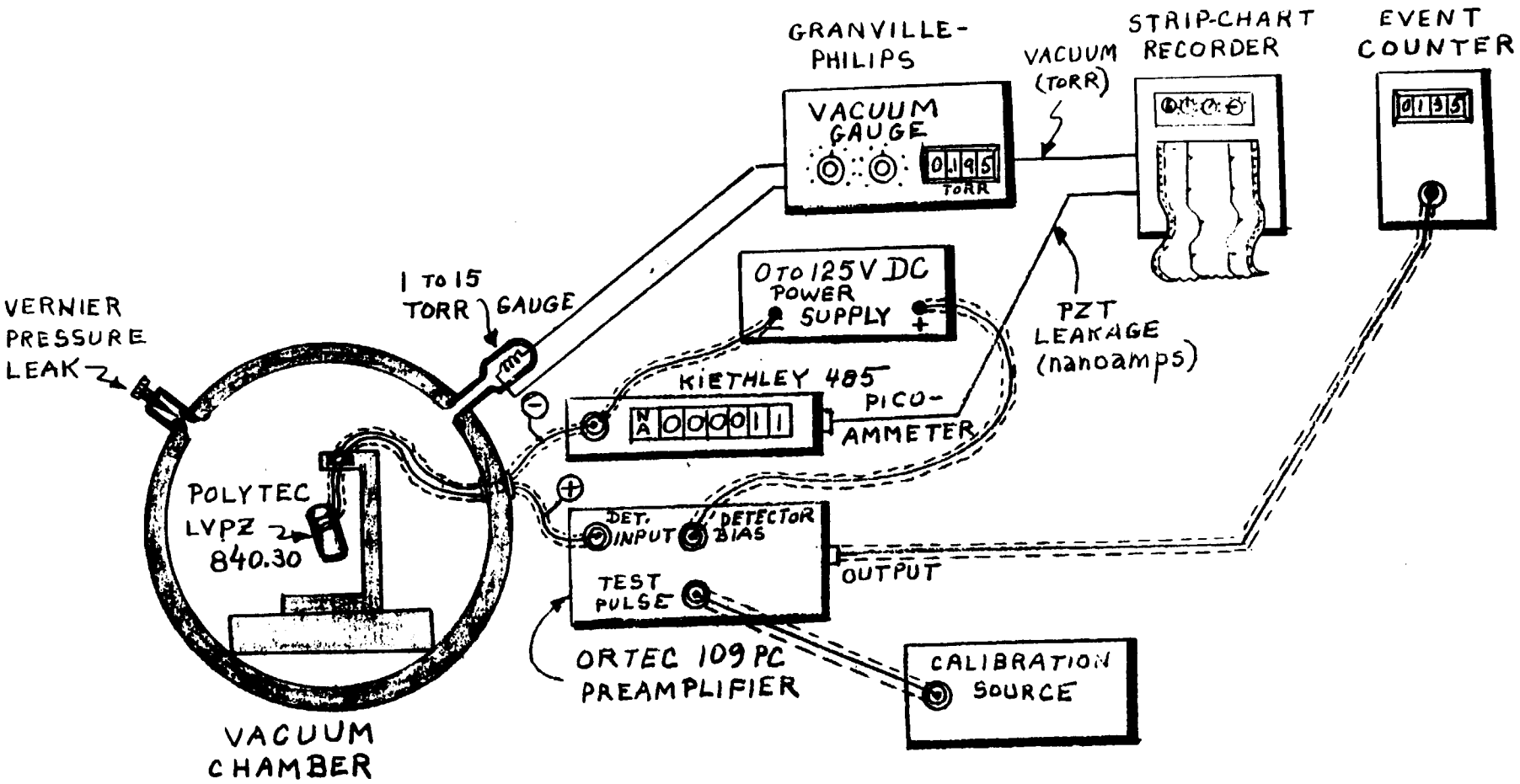

LAB. SETUP FOR PZT ALTITUDE TESTS

FIGURE 2

PZT ALTITUDE SIMULATION TEST DATA

NOTES	DATE	TIME	CHAMBER PRESSURE (TORR)	EQUIV. ALTITUDE (FEET)	VOLTAGE APPLIED TO PZT	LEAKAGE CURRENT (NANOAMPS)
START TESTS	3-29-90	0920	15	87,650	50VDC	9.44
RAISED BIAS TO 75V DC.		1430	14	89,950	75	19.95
		1730	15.5	87,550	75	20.36
RAISED BIAS TO 100V DC	3-30-90	0540	20	82,500	75	19.00
		0600	14	89,950	100	30.00
		0700	14	89,950	100	29.81
		1100	14	89,950	100	28.95
RAISED BIAS TO 125V DC		1300	16	85,400	125	41.68
REDUCED BIAS TO 75VDC		1315	14	89,950	75	18.50
PUMPED DOWN TO 10 TORR	3-31-90	0545	10	97,500	75	18.00
RAISED BIAS TO 100V DC		0830	10	97,500	100	30.50
	4-2-90	1400	9.0	99,000	100	30.50
LOST LAMBDA POWER SUPPLY	4-3-90	0342	10	97,500	Ø	—
Replaced with HP6448		0715	10	97,500	100	30.50
		0825	10	97,500	100	30.50
		1250	10	97,500	100	30.50
		1430	10.5	98,500	100	31.00
RAISED BIAS TO 125V DC		1455	10	97,500	125	46.00
		1900	10	97,500	125	47.00
	4-4-90	0620	10	97,500	125	46.60
PUMPED DOWN TO 5 TORR		0910	5.0	113,000	50	12.00
		1330	5.0	113,000	50	10.00
		1410	5.0	113,000	50	11.00
• TESTS STOPPED TO RECALIBRATE EQUIPMT.		1415	5.0	113,000	Ø	—
• ADDED GROUNDS and MORE SHIELDING -						
• PRESSURE RETAINED AT 5 TORR.						

FORM LAC 3

WORK SHEET

APPENDIX 1

PZT ALTITUDE SIMULATION TEST DATA

NOTES	DATE	TIME	CHAMBER PRESSURE (TORR)	EQUIV. ALTITUDE (FEET)	VOLTAGE APPLIED TO PZT	LEAKAGE CURRENT (NANOAMPS)
RESUMED TESTS AT	4-8-90	1745	5.0	113,000	100VDC	31.3
BIAS OF 100V DC	4-9-90	1600	4.7	113,750	100	31.3
RAISED BIAS TO 125V DC		1615	5.2	112,000	125	46.3
		1800	5.0	113,000	125	46.8
		1945	5.0	113,000	125	47.4
		2135	4.9	113,500	125	46.5
		2315	4.9	113,500	125	46.5
PUMPED DOWN TO 1 TORR		2350	1.0	153,000	50	9.2
BIAS AT 50V DC	4-11-90	0825	0.9	156,000	50	8.9
RAISED BIAS TO 75V DC		0840	1.1	150,500	75	19.8
		1215	1.0	153,000	75	18.5
RAISED BIAS TO 100V DC		1445	1.0	153,000	100	31.0
	4-12-90	1610	1.0	153,000	100	31.8
		1725	1.1	150,500	100	33.5
RAISED BIAS TO 125VDC		1730	1.1	150,500	125	49.8
		2030	1.1	150,500	125	47.6
		2140	1.1	150,500	125	45.4
		2230	1.1	150,500	125	44.6
	4-13-90	1200	1.0	153,000	125	44.5
LOWERED ALTITUDE		1205	5.0	113,000	125	44.6
		1700	5.0	113,000	125	47.8
ADDED A.C. MOD. 200Hz @95V BIAS		1835	5.0	113,000	95 DC 25 AC	33.9
		2100	5.0	113,000	95 DC 25 AC	32.4
		2200	5.0	113,000	95 DC 25 AC	31.2
END OF TESTS		2400	5.0	113,000	95 DC 25 AC	30.1

Appendix B: Manuscript for *The Astrophysical Journal*

PROPERTIES OF THE SMALLEST SOLAR MAGNETIC ELEMENTS

I. FACULAR CONTRAST NEAR SUN CENTER

K. P. Topka, T. D. Tarbell, and A. M. Title

Solar and Astrophysics Laboratory
Lockheed Palo Alto Research Laboratory, Dept 9130, B 252
3251 Hanover St., Palo Alto, CA 94304

ABSTRACT

We present measurements indicating that the continuum intensity of facular areas in solar active regions, outside of sunspots and pores, is less than that of the quiet sun very near disk center. Analysis shows that the observed continuum intensity of faculae at disk center near 5000 Å is nearly 3% less than that of the quiet sun. The intrinsic value must be even lower than this due to our finite resolution. The continuum contrast increases rapidly away from disk center, reaching +2% at 45°. The zero-crossing point, where the contrast changes sign, occurs at 20° heliocentric angle. This is contrary to many earlier observations. The photometric data were obtained using the Lockheed tunable filter instrument at the Swedish Solar Observatory, La Palma. Filtergrams of 4 active regions from 1988, 1989, and 1990 are presented. These were taken with a CCD camera, and include continuum images of very high spatial resolution (up to 0.3″), and magnetograms (up to 0.45″), which have been registered to an accuracy of better than 0.1″.

These results are sensitive to the size of the magnetic flux tubes comprising faculae, to their inclinations from local solar vertical at the $\tau(5000) = 1$ level, and to the distribution of sizes of the flux tubes. The constraint these observations place on the size of flux tubes depends upon the value of the zero-crossing point. This is important because it is independent of our resolution. Furthermore, because the contrast is changing rapidly near disk center, the zero-crossing point is well determined. Our results indicate that most of the flux tubes in solar faculae may be very small, in the range 50-100 km in diameter. The results presented here also indicate that inclination from local vertical of about 10° at the photosphere is common on the Sun. Footpoints of opposite polarity tend to tilt toward one another.

Subject headings: Sun: faculae – Sun: magnetic fields – Sun: plages

1. INTRODUCTION

Within active regions, outside of sunspots and pores, nearly all magnetic fields in the low photosphere of the Sun are concentrated into fine structures at or below the resolution limit of observations (~ 1″, see Harvey 1977 for a review). Recent observations have

confirmed and extended these results, showing that the smallest magnetic elements are still too small to be observed directly, have field strengths of order $\sim 2000 - 2400$ G at $\tau = 1$, and $\sim 1200 - 1400$ G at $\tau = 0.1$, with diameters of order 100 km (0.14″, see reviews by Muller 1985, and Stenflo 1989, see Zirin 1988 for a dissenting view). This has led to the concept of the small flux tube, an unresolved region of strong magnetic flux surrounded by practically field free plasma. Models have been developed for these small flux tubes in order to predict their properties (eg. Spruit 1976; Deinzer *et al.* 1984a,b; Hasan 1985, Steiner *et al.* 1986; Knölker *et al.* 1988; Grossmann-Doerth *et al.* 1988; Knölker and Schüssler 1988).

Faculae are bright structures seen in the photosphere that are associated with magnetic fields. They are especially visible in the continuum near the limb, but are also visible at disk center on filtergrams taken in photospheric lines. Faculae are cospatial with chromospheric plage as seen in the wings of strong chromospheric lines such as Hα and Ca II H and K. At very high resolution the faculae consists of many small continuum bright points, usually smaller than 0.5″, that are also called facular points or filigree. Larger structures, including bright facular granules and dark magnetic knots, are present in the faculae as well. The small bright points can be isolated from each other or can be clumped into chains and ring-like structures also called 'crinkles' (Dunn and Zirker 1973). Isolated bright points usually reside in intergranular lanes at the junction of 3 or more granules, and have a lifetime of about 20 minutes (Muller 1983). All of these observed phenomena, a veritable solar zoo, probably owe their existence to the small flux tube. Its properties are also important to our understanding of active region evolution, the interaction between convection and magnetic fields, and the heating of the chromosphere and corona.

Title *et al.* (1990) find, from comparison of very high resolution continuum images and accurately registered simultaneous magnetograms, that at the limit of their resolution (~ 0.35″), and registration (0.1″), the continuum bright points (filigree), line center bright points, and magnetic features are coincident. The relationship is not one-to-one, however; every line center bright point has an associated magnetic feature, but many magnetic features do not have associated bright points, in either continuum or line center, especially at high magnetic filling factors. Title *et al.* (1991, hereafter Paper 1) studied the properties of magnetic areas in an active region using simultaneous continuum, line center, Dopplergram, and magnetogram movies over 2 hours long. The observations reported in Paper 1 are very well suited to measure accurately the continuum intensity contrast of faculae. These data consist of continuum images (near Ni I 6768 Å) of very high resolution of a region of dense plage, with simultaneous and accurately registered magnetograms. Because these data exist as movies over 2 hours long, the effects of the 5-minute oscillation on intensity measurements can be understood and removed. The results, as reported in paper 1, is a contrast of -0.7% at $\theta = 14°$ heliocentric angle ($\mu = cos\ \theta = 0.970$). These results are for one image only.

In this paper we extend measurements to include 10 continuum frames from the movie data of paper 1, centered on the reference frame. The result is an average contrast of -1.0% for the faculae. Also, in this paper we report on new measurements made with the same instrument on 3 other active regions, one in 1989 and 2 in 1990. These data span the range 2.75° to 45° from disk center, and are of equal or higher resolution than those of Paper 1. Furthermore, measurements were made at three new continuum wavelengths (5250 Å , 5576 Å, and 6302 Å). The results indicate that the observed continuum intensity contrast of faculae is nearly -3% at disk center, increasing rapidly to 0% at about 20°, and then to $+2\%$ at 45°. This may indicate that the flux tubes are very small in diameter. These results are also sensitive to any non-zero inclination of the flux tubes from local vertical. In fact, the measurements presented here reveal one example of strong inclination ($\sim 35°$)

from vertical in a facular area just outside a sunspot, and suggest that smaller inclinations from vertical ($\sim 5° - 15°$) may be quite common in facular areas. In this paper we use the terms facular areas and plage areas interchangeably.

In section 2 we describe our instrument and observations. In section 3 we present our results. In section 4 we discuss the interpretation of our results, in terms of flux tube size and inclination, and compare with existing models of small flux tubes. Finally, a summary of our results and conclusions is presented in section 5.

2. OBSERVATIONS

The Lockheed tunable filter instrument used at La Palma is an engineering evaluation model of the Coordinated Instrument Package under development for the NASA Orbiting Solar Laboratory. This instrument consists of a high-speed steering mirror for image stabilization, reimaging optics, a polarization analyzer, a blocking filter wheel, a narrow bandpass (75 mÅ) tunable filter from the NASA Solar Optical Universal Polarimeter (SOUP) telescope, and a 1024 × 1024 pixel CCD camera that uses a Texas Instruments virtual phase detector (Title *et al.* 1990). The CCD camera is extremely linear. Data recording is limited by the tape drive to 246 kbytes/s. Therefore, we recorded only 512 × 512 pixels, usually by extraction from the center of the CCD, to speed up the data cycle to about 3 seconds per image.

All observations were made with this instrument at the Swedish Solar Observatory on La Palma in the Canary Islands. The site, located at 7,900 ft. at the edge of a volcanic caldera, often has exceptional seeing and the 50-cm refracting vacuum tower telescope is of excellent quality optically (Scharmer 1985, 1989). Table 1 summarizes the dates and targets for the observations reported here.

Table 1

Solar Active Regions Observed						
DATE	TIME (UT)	TARGET (NOAA)	LOCATION	θ (deg)	λ (Å)	SCALE ("/pixel)
09-29-88	10:07	AR 5168	N18 W00	14	6768	0.166
07-03-89	09:15	AR 5572	S18 E34	43	6302	0.137
06-06-90	08:25	AR 6085	S04 W02	5	5250	0.137
					5576	
06-07-90	07:57	AR 6086	N23 W19	27	6302	0.274

The first three observations have fields of view of 85" or 70", too small to include an entire medium-sized active region. The observations of 1988 September 29 and 1990 June 6 include large amounts of plage of just one polarity, and 1989 July 3 is centered on a large sunspot. Although the 1990 June 7 observation has a larger pixel size (0.274"), which means lower spatial resolution, it also means a larger field of view (140"), that allowed us

to include significant amounts of plage of both polarities. This is why this observation was included.

The observing sequence varied for each of these observations, according to the prime science objective chosen by the observer. Each observing sequence had in common the following: one left and right circularly polarized pair (LCP and RCP) in Fe I 6302 Å for longitudinal magnetograms; a five point line scan (−90, −30, 0, +30, +90 mÅ) in Fe I 5576 Å or Ni I 6768 Å for Dopplergrams, or a longer scan in Fe I 6302 Å for the determination of Stokes V; and at least one frame in the continuum. Exposure times were typically 0.2 seconds.

3. RESULTS

(A) INITIAL REDUCTION

A time interval was selected for each day when the atmospheric seeing remained excellent for at least one, and preferably three, complete cycles of the sequence. The images are corrected for gain variations and dark current, and are carefully registered and destretched into one another. Destretching removes some differential image motion across the field of view caused by atmospheric seeing (Topka *et al.* 1986). The challenge here is that the magnetogram images (taken in the blue wing of Fe I 6302 Å) do not show structures in common with continuum images, meaning that direct destretching is not possible. Therefore, intermediate destretchings are required. The intermediate images consist of a line scan, in λ 5576 Å or λ 6302 Å , made such that each image can be registered and destretched onto its nearest neighbor.

Then magnetograms were formed from each pair of blue wing images in the usual way:

$$M = \frac{k_M(I_{RCP} - I_{LCP})}{(I_{RCP} + I_{LCP})} \quad (1),$$

where I_{RCP} and I_{LCP} are the images taken in left and right circular polarization, respectively, and k_M is the calibration (estimated to be 10,000 G). In order to reduce noise, each magnetogram is the average of at least 4 individual subtractions, a minimum of 8 filtergrams. This is why more than one complete cycle of the observing sequence is required.

Precise photometry requires careful data analysis, because our "flat field" is not perfectly flat and is time dependent. Flat fields were approximated either by defocusing the instrument or by reimaging the telescope pupil onto the CCD camera. Some of the change in the flat with time is caused by the increasing temperature of the tunable filter during the day. Therefore, a second correction was needed to remove residual large scale variations in the flat field. This was done by assuming that the intensity in quiet sun over a sufficiently large area is constant over our field of views. This means we have neglected limb darkening, which is negligible for the two observations closest to sun center, and small for the observations at 27° and 43°. Figure 1 shows the resulting continuum and magnetogram images from June 6, 1990.

Some of our continuum images also have edge effects, due to vignetting. This was corrected simply be masking out those pixels nearest to the edge of the image, Usually 16 rows and columns were eliminated, leaving a 480 × 480 pixel image

Next, all sunspot umbrae and penumbrae were eliminated by masking out rectangular

areas of the image. Then pores were eliminated by constructing a pore mask using a simple threshold, where all continuum image pixels below a certain threshold were set to zero. Because of our very high spatial resolution we are able to completely eliminate any effects on our measurements by sunspots and pores. Because the tunable filter has a very narrow bandpass and was tuned to clean continuum, the effects of spectral line emission is also negligible.

The resulting spatially congruent and photometrically corrected images allow for a pixel by pixel comparison of longitudinal magnetogram signal and continuum intensity. Using the magnetograms as a mask, and choosing a bin size of 25 G, we have calculated the mean continuum intensity contrast as a function of magnetogram signal ($C(M)$) for all four observations. $C(M)$ is defined as:

$$C(M) = \frac{< I_{pl}(M) >}{< I_{qs} >} - 1.0 \qquad (2),$$

where $< I_{pl}(M) >$ is the average continuum intensity in a facular area (plage) at a magnetogram signal M, and $< I_{qs} >$ is the same average for quiet sun (mean of all continuum image pixels with corresponding magnetogram signal between -12 and $+12$ G inclusive). The results for all four observations are shown in Figure 2. The labels on the plot refer to the mean angular distance θ for each observation from disk center: 1990 June 6 (5°), 1988 September 29 (14°), 1990 June 7 (27°), and 1989 July 3 (43°). Since the magnetogram measures only the line-of-sight component of the field, it was corrected by dividing by $cos\ \theta$. Note that for the two measurements made closest to disk center (5° and 14°), $C(M)$ is negative for all non-zero values of the magnetogram signal. Also notice the knee in these measurements at about 700 G. Above the knee $C(M)$ drops much more rapidly then below, even with all pores removed. For the other two observations, further from disk center, there is a substantial range of magnetogram signal where the contrast is positive.

The contrast of the faculae is C_{pl}, where:

$$C_{pl} = C(188 - 612G) \qquad (3).$$

The lower limit of 188 G was chosen to be at least 3σ above 0 G (noise level is about 50 to 60 G per pixel, and 187.5 G represents the boundary between two bins 25 G wide). The upper limit of 612 G was chosen to be below the knee revealed in Figure 2. This is where we expect the smallest flux tubes to reside. Note that this definition for C_{pl} is not the same as the peak in the curves shown in Figure 2, and that it tends to favor lower magnetogram signals, since our magnetograms tend to have more pixels with 200 G then with 600 G. This number is the fundamental measurement reported in this paper. It is discussed in various parts of this paper as a function of heliocentric angle, of time, and for different polarities.

(B) ESTIMATE OF MEASURING ERROR

The uncertainty in our measurement of C_{pl} is caused principally by atmospheric seeing, CCD signal to noise ratio and counting statistics, scattering of light within the field of view, and systematic errors in the flat field. The effects of seeing, and of CCD S/N ratio and counting statistics, can be estimated by repeating the same measurement several times. Such measurements are available from 1988 September 29, the data used for paper 1, because we produced movies from these data. Figure 3 shows C_{pl} versus rms contrast of

the quiet sun. The *rms* contrast of the quiet sun varies directly with atmospheric seeing. There is a suggestion of a trend in Figure 3 (correlation coefficient -0.53) as expected. When the resolution is higher (*rms* is larger), the contrast is also higher. There is a lot of scatter about this correlation because we expect other phenomena, such as 5-minute oscillations, to influence these measurements. Using the straight line fit in Figure 3, we have made approximate corrections to C_{pl} for atmospheric seeing. The mean value for all of these measurements is then -1.00%, with a scatter of about 0.5% peak to peak, and 0.25% rms. Since there are twenty measurements, the error in the mean is $0.25/\sqrt{20}$, or $\pm 0.06\%$.

The observations used in Figure 3 have a quiet sun *rms* contrast of 4.5% at best, and were obtained at 6770 Å. Figure 1(a) has a quiet sun *rms* contrast of 6.0% at 5580 Å. Using the wavelength variation of the *rms* from Bray, Loughhead, and Durant (1984), these measurements are equivalent to 7.1% and 7.8% at 4300 Å, respectively. The best granulation pictures taken at La Palma, using a video CCD camera and video image selection system, have *rms* contrast of about 10% at 4300 Å (Scharmer 1990).

The effects of systematic errors in flat fields can be determined by repeating measurements of C_{pl} at different wavelengths which use different flat fields. The 1990 June 6 observation includes filtergrams in the continuum at 5250 Å and 5576 Å, taken just a few seconds apart in nearly identical atmospheric seeing conditions, and reduced using two different flat fields. The difference in C_{pl} is 0.33%, which provides an estimate for the uncertainty in our measurement due to flat field. This difference is much larger than is obtained from nearly identical frames reduced with the same flat field. For example, our data from 1990 June 7 consists of 2 continuum frames taken about 3 seconds apart in nearly identical seeing conditions, and they have the same flat field. The measured C_{pl} for these two frames are nearly identical; +0.92% for frame 1 and +0.93% for frame 2.

We have divided 10 images from the continuum movie of 1988 September 29 into 16 sub-images each (120×120 pixels), and then processed each sub-image separately to find $C_{pl}(+)$ (positive polarity). Because of fewer pixels the statistical accuracy of the measurement is lower than that for a full frame, but the quiet sun and plage areas used to calculate C_{pl} are located close by within each small field of view. Figure 4 shows the results. The mean value of $C_{pl}(+)$, determined from all 16 subimages in all 10 frames, is $-1.11 \pm 0.07\%$ $(0.88/\sqrt{160})$. When $C_{pl}(+)$ is determined for the entire field of view, the mean is -1.00 ± 0.06 % $(0.23/\sqrt{10})$. These results are in good agreement, and this eliminates the possibility of many types of systematic errors in the flat field. Table 2 gives our estimates of the errors in our measurements.

Even with a perfect instrument we are limited in the precision to which we can measure C_{pl}. This is due to bright point intensity variations, 5-minute oscillations, noise due to granulation, and the fact that isolated small flux tubes preferentially lie in intergranular lanes. Up to 35% of all the continuum intensity fluctuations seen in SOUP white light movies were due to 5-minute oscillations, not granulation (Title *et al.* 1989). Furthermore, the amplitude of the 5-minute oscillation is reduced in magnetic areas, when compared to quiet sun. Therefore, we expect them to influence these measurements. We estimate from Figure 3 that the effect of 5-minute oscillations on a single measurement is about $0.2-0.3\%$.

Auffret and Muller (1991) directly measured a mean contrast of +8.5% for network bright points at disk center. Their measurements range from -2% to +25%, a large dispersion they explain as due to a variation in brightness during bright point lifetime. These results

are not corrected for instrumental resolution (at least 0.23″). Since these bright points are probably due to small flux tubes, such variations will have an important influence on measurements of C_{pl}, especially if attempted over a small area.

Table 2

Estimate of Probable Error	
Measurement area	Error (1σ)
128 × 128 pixel subimage	±0.9%
512 × 512 pixel image	±0.4%
2 images, 2.5 min apart	±0.2%
10 images	±0.1%

(C) VARIATION OF CONTRAST WITH HELIOCENTRIC ANGLE

The heliocentric angles (θ) of our observations were determined by comparison with KPNO full disk magnetograms, taken on the same day and rotated backwards to correspond to our time of observation. Figure 1 shows the 1990 June 6 observation with the images rotated such that north is on top, east is to the left. The arcs seen superimposed on these images represent heliocentric angles of 3°, 5°, and 7°. These images have been divided into angular bins 1° wide. Each bin was treated like a separate image, with $C_{pl}(\theta)$ being determined independently. The 1988 September 29 observation (11.5° to 15.5°) was divided into bins 2° wide. We did this to better constrain the behavior of C_{pl} near disk center, where the new results of this paper are obtained.

Table 3 lists our measurements of C_{pl} with heliocentric angle for both positive and negative polarity, and they are plotted in Figure 5. This figure also shows a dashed curve representing our estimate of the smooth trend in these data. This curve (a polynomial fit of order 2) shows that C_{pl} may be as low as −2.8% at sun center, that it increases rapidly with angle to 0% at about 20°, and that it reaches +2.1% at 45°. As shown in the third column of Table 3, each measurement is the average of 2 continuum frames, except 1988 September 29, which is the average of 10 frames. Note that the deviation of some of individual data points from the smooth trend is larger than our estimate of the measuring error (Table 2). As discussed in section 4(b), we believe that some of this is due to inclination effects. The total change (5%) is more than 12 times larger than the measuring uncertainty as estimated in Table 2.

4. ANALYSIS

(A) PREVIOUS OBSERVATIONS

Our results (Table 3, Figures 2 and 5) are at variance with many earlier observations of C_{pl} near disk center. Foukal and Fowler (1984) obtained a value of +0.1% near sun center, using a technique very similar to ours. Their Figure 3 resembles our Figure 2,

Table 3

Variation in Contrast with Heliocentric Angle						
ANGLE (DEG)	DATE	N	NEG PIXELS	$C_{pl}(-)$ (NEG)	POS PIXELS	$C_{pl}(+)$ (POS)
3.0-4.0	06-06-90	2	1615	-0.09	1902	-2.35
4.0-5.0	06-06-90	2	651	-2.55	14296	-1.84
5.0-6.0	06-06-90	2	2305	-1.81	12011	-1.92
6.0-7.0	06-06-90	2	1888	-2.74	3013	-0.78
11.5-13.5	09-29-88	10	6265	-0.55	11197	-0.84
13.5-15.5	09-29-88	10	1169	-0.26	24748	-1.05
25.2-28.6	06-07-90	2	-	-	3364	+0.93
25.4-28.8	06-07-90	2	4292	+0.69	-	-
40.6-46.3	07-03-89	2	7065	+1.99	10663	+1.95
43.4-45.9	07-03-89	2	11507	-1.53	2445	+3.31

although their spatial resolution is much lower (1″ pixels), and therefore the magnitude of their signal is smaller. Hirayama *et al.* (1985) obtained +0.04% for C_{pl} at disk center after averaging over their three innermost bins. Although their photometric accuracy is very high, their spatial resolution is very low (20″), and they do not have simultaneous magnetograms. Lawrence (1988) obtained positive contrast of a few tenths of one percent for faculae at sun center. His detector consisted of a one dimensional 512 element array, and it was operated in raster mode. Images with about 1″ pixels were made in continuum in green, red, and infrared, as well as at Ca II 8662 Å to identify facular areas. Lawrence, Chapman, and Herzog (1988) obtained +0.74% ± 0.11% for the disk center contrast at 8660 Å. Lawrence, Chapman, and Walton (1991) obtained a value of about +0.2% near disk center. Their observations nearest disk center actually include 5 images over three days, and span the range $0.79 < \mu < 0.97$. Since our measurements indicate that C_{pl} reverses from negative to positive for $\mu > 0.94$, most of their observations were made too far from disk center to obtain the same results.

We cannot explain all the difference between these earlier results and ours. We note that the magnitude of our result at sun center is 10 times or more larger than most of these previous observations, probably due to our higher resolution. We also note that our magnetograms are simultaneous with our continuum images within 30 s, and our estimate of our registration accuracy is about 0.1″. In any case, the apparent discrepancy has motivated us to be very careful in our data reduction. We have also repeated these observations on about 20 active regions from center to limb, with the same instrument at La Palma during the summer of 1991. Details of our results will appear in future papers, but we can state here that the analysis of one 1991 observation near disk center (1991 August 11, 16:24 UT, $\theta = 10°$) agrees with our results that C_{pl} near disk center is

negative.

C_{pl} is determined from all image pixels with magnetogram signal between 188 and 612 G. In this area the filling factor is (~ 0.1 to ~ 0.5), since the intrinsic magnetic field strengths in faculae are approximately 1200 to 1400 G. This implies that our measurements are dominated by the immediate surroundings of the small flux tubes. The small flux tubes are bright, but the immediate surroundings are dark. It is known that small flux tubes are located preferentially in dark intergranular lanes. This may provide an explanation for why the contrast of faculae is negative at disk center in our observations.

This simple explanation has two severe difficulties. First, C_{pl} changes very rapidly with heliocentric angle near disk center, increasing by 3% from disk center to 20°. However, the properties of intergranular lanes do not change near disk center, as determined by the *rms* contrast. For example, at 20° the small flux tubes would still appear to be inside intergranular lanes, and the lanes still appear dark. According to Keil (1977) the *rms* contrast of granulation changes negligibly within about 35° of disk center. If intergranular lanes dominate the photometry, C_{pl} would remain negative at 20°, and probably out beyond 35°. This is not observed. Second, our results are dominated by facular areas in which the granulation is abnormal (see Figure 11). Granules and intergranular lanes are smaller in abnormal granulation, and are probably not fully resolved in our observations. Only isolated flux tubes reside in large intergranular lanes at the junction of 3 or more well developed granules.

Foukal *et al.* (1989, 1990) report that the contrast of some facular areas near disk center is negative in the infrared (1.63μm). These observations are made where the H^- opacity is at a minimum, so the deepest layers are seen. The darkest IR structures present in their images outside of sunspots and pores have observed contrast of about -2%. They seem to correspond to areas of brightest plage. Other areas within the plage have IR contrast indistinguishable from zero. It is possible that the darkest IR structures correspond to areas of strong magnetogram signal, where larger flux tubes that are dark dominate (see section 4d). Note from Figure 2 that the visible contrast can be as low as -12% at 1200 G at our resolution. The difference between -2% and -12% may be due to the lower spatial resolution of the IR observations. The areas within the plage that have IR contrast indistinguishable from zero possibly correspond approximately to areas with weaker magnetogram signal, where we determine C_{pl}.

(B) INCLINATION OF THE FLUX TUBES

Our observations show that the continuum contrast of faculae changes rapidly with heliocentric angle ($C_{pl}(\theta)$). We assume that this change is a function solely of the angle between the line of sight and the lines of force at the continuum, because we believe that the physical properties of the magnetic elements in all of our observed facular areas are the same. This assumption implies that our observations are sensitive to any inclination from solar vertical of the lines of force in the facular flux tubes at the continuum. Suppose that all of these tubes are exactly vertical at the continuum. Further suppose we have a small simple bipole with leading and following polarity separated by (20″), oriented west-east, that passes across the disk 10° north (or south) of the equator. Using the smooth polynomial fit for $C_{pl}(\theta)$ of Figure 5, we can calculate the difference in contrast expected between the leading and following polarities ($\Delta C_{pl} = C_{pl}(l) - C_{pl}(f)$) as a function of longitude of the center of mass of the bipole. The results are the solid line shown in Figure 6, and labeled 0°. Notice that ΔC_{pl} is negative in the east and positive in the west. This is because in the east the heliocentric angle of the l-polarity is always less then that for the f-polarity, and therefore from Figure 5 we know that $C_{pl}(l)$ must always be less than

$C_{pl}(f)$. Just the opposite is true in the west.

Now assume that the lines of force are no longer vertical, but are inclined such that the l- and f-polarities of the bipolar region tend to point toward one another. Curves of ΔC_{pl} as a function of longitude for inclinations of 3°, 6°, and 9° from local solar vertical are also shown in Figure 6. This figure reveals that by using ΔC_{pl} to detect inclination, the greatest sensitivity in our observations occurs about 1/2 day before or after meridian transit, and that inclinations exceeding about 6° should be readily detectable in a single observation.

All of our observations contain at least some plage of both polarities. This means we can measure ΔC_{pl} between plage of opposite polarity ($\Delta C_{pl} = C_{pl}(+) - C_{pl}(-)$) for nearly the same heliocentric angle. We interpret $\Delta C_{pl} = 0$ to mean that there is no relative inclination between plages of opposite polarity, which probably indicates that the flux tubes are vertical (although they still could be both inclined the same amount in the same direction). Using $\Delta C_{pl} \neq 0$ as the criterion, however, examples of non-zero inclination were detected in all observations.

The largest inclination was detected in the negative polarity plage of AR 6086 (1989 July 3), just limbward of the main sunspot. Using the entire field of view we obtained $C_{pl}(+) = +1.95\%$. These measurements are shown in Figure 2 and Table 3. The heliocentric angle of this observation ranges from 40.6° to 46.3°. However, $C_{pl}(-)$ for the full field is -0.2%. The resulting ΔC_{pl} is +2.15%, far larger than can be explained by instrumental effects or measuring error. We examined the continuum images (there are 2) for this observation, using the registered magnetogram as a mask to include only areas with magnetogram signal between -600 and -200 G. We discovered that there were two broad regions within the image, one where the continuum in the negative polarity plage was obviously bright, while in the other it looked very dark. Figure 7 shows the magnetogram from this observation, with a box outlining region 2, the region where the continuum looked dark. The rest of the field of view we call region 1. We then recalculated $C(M)$, and C_{pl} separately in these two regions. In region 1 we obtained $C_{pl}(-)$ of +1.99%, in excellent agreement with $C_{pl}(+)$ from the entire field (+1.95%), and included it in Table 3. These measurements are shown in Figure 8*a*, where $C(M)$ is plotted as a function of the absolute value of M so both polarities could be included on the same figure for comparison. Let us assume that the weighted average of these two measurements (+1.97%) represents the "benchmark" contrast for vertical flux tubes at this heliocentric angle (43°).

Figure 8*b* shows that $C_{pl}(+)$ in region 2 is +3.31%, the highest value observed in this data set, while $C_{pl}(-)$ is −1.53%, despite the fact that we are 44° away from disk center. Therefore, ΔC_{pl} is +4.84% for region 2, a difference that is 12 times or more larger than the uncertainty in our measurements (Table 2). These measurements are also included in Table 3, with θ ranging from 43.4° to 45.9°. From Figure 5 we see that a contrast of −1.53% is consistent with an angle of only about 8° between the line of sight and the lines of force. We interpret this result to mean that the negative polarity plage is inclined from vertical by about 35°, in the sense that the flux tubes are tilted back toward sun center. Lying in that direction is the large sunspot of opposite polarity on which the observation was centered. It is possible that some of this plage and the spot are directly connected by closed magnetic loops. The Hα images of this region, taken simultaneously, tend to support this possibility. We also see from Figure 5 that a change in contrast of 4.84% implies a relative inclination change of about 45° between positive and negative plage. Since the negative plage is inclined toward sun center by 35°, the positive plage must be inclined *away* from sun center by about 10°. This is consistent with the result that $C_{pl}(+)$ in region 2 is +3.31%, versus our "benchmark" for vertical tubes at this heliocentric distance

of +1.97%.

Other candidates of facular areas with inclined flux tubes are revealed by Figure 5. Some of the measurements of $C_{pl}(+)$ $C_{pl}(-)$ and agree ($\Delta C_{pl} \sim 0$), but others do not. The largest ΔC_{pl} occurred in the 1990 June 6 observation at $\theta = 4°$ and 7°, as indicated in Figure 5 by the vertical arrows. $C(M)$ for both polarities at $\theta = 4°$ are shown in Figure 9*a*, while $C(M)$ at 7° is plotted in 9*b*. Figure 9*a* shows that $C_{pl}(+)$ is -2.35% and $C_{pl}(-)$ is -0.09%. Therefore, ΔC_{pl} is -2.24% for $\theta = 4°$, much too large to be instrumental. Let us assume that the positive polarity flux tubes are approximately vertical. There is far more positive polarity plage in this observation than negative, so we might expect its mean tilt to be lower. Furthermore, the measured value for positive polarity comes close to the smooth fit, which has been determined from all positive polarity measurements. With this assumption we then interpret our result as meaning that the negative polarity is tilted nearly 20° away from sun center.

Figure 9*b* shows that $C_{pl}(+)$ (-0.78%), while $C_{pl}(-)$ is -2.74% for $\theta = 7°$, the lowest value we have observed yet. ΔC_{pl} (+1.96%) is almost the exact opposite obtained at $\theta = 4°$, meaning that the flux tubes are tilted in the opposite sense (negative polarity toward sun center, positive away). We assume that the negative polarity flux tubes are approximately parallel to the line of sight on average, because $C_{pl}(-)$ is the lowest contrast observed, and because it agrees well with the value of the smooth fit of Figure 5 at $\theta = 0°$. If true then the mean tilt is 7° toward sun center. Since $C_{pl}(+)$ is 1.96% larger, and positive polarity flux tubes must be tilted away from the negative polarity (and thus from sun center) by a relative angle of about 16°. Figure 6 shows the measurements of ΔC_{pl} plotted as dots. The expected values, assuming zero inclination, as also plotted in this figure as open squares. The sign of ΔC_{pl} at 7° in Figure 6 is the opposite of above because it is equal to leading minus following polarity, and the most likely location of the neutral line indicates that the negative polarity is leading.

A summary of our inclination results is shown in Table 4. Inclinations from local solar vertical range from a high of 35° to a low 6°. We listed no results less than 6° in Table 4 because this is our estimate of the limit at which we can detect relative inclination with confidence from just one observation. Howard (1991) observed mean inclinations in plage areas by measuring the difference in magnetogram signal between active regions spaced equally east and west of the central meridian. His results for about 8000 active regions indicate that on average the *l*- and *f*-polarities are inclined toward each other by about 16° (10° for *l*, 6° for *f*). This agrees well with the magnitude of the inclinations shown in Table 4. We can tell whether the inclination is toward or away from sun center, by the sign of ΔC_{pl}. Also, we can often tell the location of the neutral line, from our own magnetograms and Hα observations, as well as from the KPNO full disk magnetograms. In each case where the flux tube was inclined toward sun center, the most likely location of the neutral line was also toward sun center, and vise versa. These results are listed in Table 4. This is exactly what is expected for closed loops, where the ends of opposite polarity tilt toward each other.

The fact that inclination is so common may partially explain why earlier observations failed to obtain the correct results at disk center. If inclined from local vertical, faculae located at disk center will have much larger contrast then expected. As seen in Figure 5, this occurred in our observations for negative polarity at 4° and positive polarity at 7°. The overall effect is to partially fill in the deficit in C_{pl} near disk center.

(C) SIZE OF THE FLUX TUBES

Table 4

Inclination of Plage Flux Tubes				
AR	POL	INCLINATION (DEG)	INCLINATION DIRECTION	NEUTRAL LINE DIRECTION
6085	N	18	AWAY	AWAY
6085	N	7	TOWARD	TOWARD
6085	P	8	AWAY	AWAY
5168	N	6	AWAY	AWAY
6086	N	6	TOWARD	TOWARD
5572	P	10	AWAY	-
5572	N	35	TOWARD	TOWARD

The continuum contrast of bright points at disk center was estimated to be +20 to +40% (Frazier and Stenflo 1978, Muller and Keil 1983). Schüssler and Solanki (1988) derive a lower limit for the contrast at $\theta = 0°$ of +40%. Their results are based on the observed weakening of temperature sensitive spectral lines obtained by comparing the line profiles originating solely in the magnetic elements (by integrating the observed Stokes V profiles to produce an approximation for Stokes I) with those obtained directly with the same instrument for quiet Sun.

From these results we might expect the observed contrast of faculae near disk center to be positive, as has been obtained in many of the earlier observations. Model calculations of magnetic flux tubes, however, show that the situation is not so simple because of the expected presence of dark rings immediately surrounding each bright point (Deinzer *et al.* 1984b, Knölker *et al.* 1988, Knölker and Schüssler 1988, and Grossmann-Doerth *et al.* 1988). The magnetic structure in these models is actually not a round "flux tube", but is instead a 2-D "flux sheet" which extends only in the z-axis (vertical) and x-axis (horizontal). Models representing very small flux tubes usually predict a central bright point (some, but not all, having contrasts greater than 40%) surrounded by a dark ring in the non-magnetic Sun just outside of the flux tube. Both structures are due to the same phenomenon; the horizontal inflow of radiation into the partially evacuated tube from the surrounding non-magnetic medium. Averaging over both structures, which all existing observations must necessarily do, leads to a disk center contrast that is in fact very close to zero. For many of the models it is negative.

For several of these models the theoretical center-to-limb variation (CLV) of the continuum intensity contrast C_{pl} has been calculated. For example, Figure 11 of Deinzer *et al.* (1984b) reveals that C_{pl} for model A (size = 170 km, Wilson depression = 130 km) varies from −3% at disk center to +5% near the limb. This is for a 1″ spatial average centered on the structure. Model A is meant to represent the very smallest flux tubes on the Sun, thought to be responsible for facular points and filigree. From the CLV the zero-crossing point (θ_0, where the reversal from negative to positive contrast occurs) can be determined (49° from disk center for model A). The zero-crossing point occurs because of projection effects; the

projected area of the outer dark ring goes to zero as the flux tube approaches the limb faster than that of the inner bright point ("hot wall" effect described by Spruit, 1976). The importance of the zero-crossing point is that it is an observable quantity (easily obtained from Figure 5), that is, to a good approximation, independent of our resolution. Because of this, we can directly compare the theoretical and observed zero-crossing points.

Figure 10 shows a plot of theoretical zero-crossing point for 5 model flux tubes versus $tan^{-1}(d/Z_w)$, where d is the model flux tube diameter and Z_w is the Wilson depression. Three of the models are from Deinzer *et al.* (1984b), while two are from Knölker and Schüssler (1988). Free model parameters include ϕ, the total magnetic flux, and α, the initial ratio of internal to external gas pressure (evacuation parameter). Models are labeled in Figure 10 by the value of the evacuation parameter. All of these models predict a much larger value for θ_0 then is observed (49° or more predicted versus 20° observed). Also, Figure 10 shows that the predicted value of θ_0 is model dependent. Furthermore, these models are 2-dimensional slabs, not cylinders.

Deinzer *et al.* (1984b) argue that the comparison of observations to their models tends to favor those near equi-partition ($\alpha = 0.5$). Note from Figure 10 that they fall near the diagonal of this plot. This yields the heuristic result that $\theta_0 = tan^{-1}(d/Z_w)$, approximately valid for these models. Our observed zero-crossing point lies far outside the range covered by these models, but let us assume that this result is still valid. Note that this has a geometrical interpretation. If we assume that $\theta_0 = tan^{-1}(d/Z_w)$, and that the flux tube is a cylinder, then θ_0 is the smallest angle between the line of sight and the axis of the cylinder at which the floor of the flux tube is not visible. Applying this to our observations ($\theta_0 = 20°$) yields $d = 0.36 Z_w$. We cannot determine the value of Z_w for such small tubes independently, but it is easy to do so for sunspots. This is done by measuring the apparent size of the penumbra parallel to the solar radius on both the sun center and limbward sides as the spot rotates from center to limb. Recent results yield a value of 230 km (Collados *et al.* 1987). If we assume a Wilson depression of 200 km, then we obtain a geometrical size of about 70 km for plage flux tubes. Zayer *et al.* (1989) were able to set some preliminary constraints on the size of flux tubes from comparison of observations at two disk positions, and obtained a value of 60 - 100 km assuming a slab geometry, and about 300 km for cylindrical flux tubes.

(D) RANGE OF SIZE OF THE FLUX TUBES

Our results show that plage flux tubes come in a range of sizes. First, there is the existence of the "knee" at about 700 G in the curves of contrast versus magnetogram signal ($C(M)$, Figure 2). $C(M)$ drops much more rapidly above this point then below. Second, we note from Figure 2 that above about 850 G the contrast $C(M)$ is still negative at 43° from disk center. This suggests that the predominate size of flux tubes for $B > 850$ G is larger then for $B < 700$ G, since we know from models such as those shown in Figure 10 that larger flux tubes are expected have zero-crossing points closer to 90°. Third, we can look at the locations in the continuum images corresponding to the strongest magnetogram signals. Results for the 1990 June 6 observation are shown in Figure 11. The magnetogram has been used as a mask for the continuum image, with a threshold set at 200 G to differentiate quiet sun (11*a*) from plage areas (11*b*). The granulation appears normal in Figure 11*a*, but is quite disturbed in 11*b* (abnormal granulation), in agreement with paper 1. Eight arrows are added to Figure 11*b* to reveal the areas of strong magnetogram signal. In all cases the arrows point to dark structures in the continuum. These are often referred to as magnetic knots, and are probably flux tubes intermediate in size between the smallest magnetic elements and pores. They may resemble the models of Knölker and Schüssler (1988), since the size and contrast we measure is quite similar to the predictions of this

paper.

5. SUMMARY AND CONCLUSIONS

The principal results of this paper are presented in Table 3 and Figure 5. The continuum contrast, C_{pl}, of facular areas with magnetogram signal bewteen 188 and 612 G is a minimum at disk center (-2.8%), rising rapidly with heliocentric angle to +2.1% at 45°. The zero-crossing point, where the contrast changes from negative to positive, occurs at $\theta_0 = 20°$. This is a new result. The continuum images have a resolution of 0.3″ at best, the magnetograms 0.45″. At this resolution most of the facular flux tubes are still unresolved. The filling factor where C_{pl} is measured averages about 0.1 to 0.2, so the immediate surroundings of the small flux tubes dominate the photometry.

Models of small flux tubes predict that they are partially evacuated cavities filled with radiation emitted from the sides. The result is a central bright point surrounded by a dark ring. The entire structure appears dark when unresolved and viewed from straight overhead, but bright when viewed from the side. Our observations support this prediction. Isolated small flux tubes are known to reside preferentially within intergranular lanes. We do not believe that this can explain our results. This is because C_{pl} changes very rapidly with heliocentric angle near disk center, whereas the *rms* contrast of granulation does not.

We have attempted to compare our observations with models of small flux tubes, principally by using the zero-crossing point (θ_0). The importance of θ_0 is that it is well determined from our observations due to the rapid change in C_{pl} near disk center, and is also independent of our resolution. All existing models predict values of θ_0 much larger then is observed (20°), leading us to believe that the typical facular flux tube is very small in diameter. Assuming the heuristic result $\theta_0 = tan^{-1}(d/Z_w)$, the diameter is about 70 km for a Wilson depression of 200 km.

A more detailed analysis than this must await the development of models with smaller diameters. In particular, we note that existing models are 2-dimensional. Since the geometry of the tube may greatly influence the relative structures of the central bright point and surrounding dark ring, we recommend that full 3-dimensional models be constructed, starting with cylindrical shaped flux tubes. We have not attempted to correct our measurements for finite resolution. This is because the correction is probably large, and requires knowledge of the telescope MTF (modulation transfer function, which we know only approximately), and of the atmospheric MTF (which we do not know). It is more accurate to smooth the model predictions with a 0.4″ FWHM PSF (assumed gaussian) for comparison with these observations.

We can determine the mean inclination from vertical of the lines of force in small flux tubes from these data (Table 4, Figures 8 and 9). The assumption we need make is that C_{pl} for a sufficiently large number of flux tubes is solely a function of the angle between the line of sight and the lines of force. This is equivalent to assuming that the flux tube size spectrum within 188 to 612 G is the same in all regions of all observations. From the results shown in Figure 6 and Table 2 we estimate that inclination exceeding about 6° from local vertical is detectable in from single observation. This technique is sensitive only to the component of inclination along a radius joining the faculae with sun center. A higher precision in measuring C_{pl}, and therefore inclination, may be obtained by averaging several individual measurements. Vector magnetic observations are incapable of detecting such small deviations from vertical.

It is unlikely that all contrast changes are due to inclination. Foukal (*et al.* 1990) observe

substantial differences in contast within facular areas at 1.63 μm, and argue that these are likely due to variations in flux tube size. Knölker and Schüssler (1988) find that flux tubes with diameters larger of 500 *km* or more are dark in their interiors. They appear dark when viewed at disk center, while still appearing bright at the limb. We conclude that size difference cannot explain all of our observations because our contrast measurements are made in the 188 to 612 G range, where we believe that small flux tubes dominate. In our magnetograms large flux tubes, such as those in Figure 11b, almost always show magnetogram signels larger than 600 G. Furthermore, if all contrast changes we observe are due to size variations, the correlation between inclination direction and neutral line direction, as shown in Table 4, would not exist.

We conclude that the lines of force in facular flux tubes are often inclined from vertical by about 10°, in the sense that footpoints of opposite polarity are tilted toward each other. This result agrees well with those of Howard (1991). The degree of inclination, which varies from about 6° to 35°, may depend on the size and shape of the closed loop. We expect our more extensive observations (made at La Palma in 1991, to appear in future papers) to confirm and extend this result.

Our results are consistent with the notion that plage flux tubes exist in a wide range of sizes. At low magnetogram signals (up to the knee at 700 G), very small magnetic flux tubes seem to predominate. The best evidence for this is the rapid change of C_{pl} from negative to positive near disk center. Above about 850 G the contrast is still negative at 43° heliocentric angle, implying that the flux tubes here are significantly larger than those occurring below 700 G. Even more important, dark structures in the continuum resembling magnetic knots are often observed to be spatially coincident with areas of strong magnetogram signal.

The magnetic knots range in size in our observations from about 250 km (close to the resolution limit), to nearly 1500 km. The continuum bright points we see tend to be smaller than this. Therefore, our observations tend to support the prediction that small flux tubes are bright, while larger ones are dark. A similar conclusion was reached in paper 1. Magnetic knots may resemble pores in structure, except that they have less total magnetic flux (therefore are smaller in size), and have contrast closer to quiet sun (-15% to -25% for magnetic knots, approximately -50% for pores). It is not likely that magnetic knots are a close association of very small but distinct flux tubes, as was suggested by Knölker and Schüssler (1988). The smallest flux tubes are bright in the center, with surrounding dark rings. Therefore, a close association of these structures must occasionally have a bright point at its center that is large enough to be seen at our resolution. Magnetic knots are always darkest at their centers.

Observations made with the ACRIM and ERB radiometers onboard the *SMM* and *Nimbus 7* spacecraft showed that the solar irradiance, S, varies by about 0.15% during the solar cycle, in the sense that S is a maximum around sunspot maximum (Hudson 1988; Hickey *et al.* 1988). Furthermore, these same instruments showed that shorter term variations in S are linked to sunspots (which contribute negatively) and bright photospheric magnetic elements (which contribute positively; Oster *et al.* 1982; Livingston, Wallace, and White 1988; Foukal & Lean 1988; Chapman *et al.* 1989). Our results show the value of our instrument and techniques to the study of solar variability. The contribution that faculae make to the solar luminosity is the integral of their radiation pattern over 2π steradians, and is thus sensitive to the center-to-limb variation in contrast.

Acknowledgements

These observations were obtained at the Swedish Solar Observatory, La Palma. We thank Dr. Gören Scharmer, director, and the staff at the observatory for their support, especially Rolf Kever and Paco Armas. Many people at Lockheed contributed to the success of this program, including Dexter Duncan, Christopher Edwards, Stuart Ferguson, Zoe Frank, Kathy Hwu, Michael Levay, Michael Morrill, Roger Rehse, William Rosenberg, Richard Shine, Kermit Smith, and Darrel Torgerson. This work was supported by Lockheed Independent Research Funds, by the Swedish Royal Academy of Sciences, and by NASA contracts NAS8-32805 (SOUP), NAS5-26813 (OSL), NAS5-30386 (MDI), and NAS8-38106 (BSOUP), and NSF contract ATM-8912841.

REFERENCES

Auffret, H., and Muller, R. 1991, *Astr. Ap.*, **246**, 264.

Bray, R. J., Loughhead, R. E., and Durrant, C.J. 1984, *The Solar Granulation*, (Cambridge: Cambridge Univ. Press), p. 71.

Chapman, G. A., Herzog, A. D., Laico, D. E., Lawrence, J. K., and Templer, M. S. 1989, *Ap. J.*, **343**, 547.

Collados, M., Del Toro Iniesta, J. C., and Vazquez, M. 1987, *Solar Phys.*, **112**, 281.

Deinzer, W., Hensler, G., Schüssler, M., and Weisshaar, E. 1984a, *Astr. Ap.*, **139**, 426.

Deinzer, W., Hensler, G., Schüssler, M., and Weisshaar, E. 1984b, *Astr. Ap.*, **139**, 435.

Dunn, R. B., and Zirker, J. B. 1973, *Solar Phys.*, **33**, 281.

Frazier, E. N., and Stenflo, J. O. 1978, *Astr. Ap.*, **70**, 789.

Foukal, P., and Fowler, L. 1984, *Ap. J.*, **281**, 442.

Foukal, P. V., and Lean, J. 1988, *Ap. J.* **328**, 347.

Foukal, P., Little, R., and Mooney, J. 1989, *Ap. J.*, **336**, L33.

Foukal, P., Little, R., Graves, J., Rabin, D., and Lynch, D. 1990, *Ap. J.*, **353**, 712.

Grossmann-Doerth, U., Knölker, M., Schüssler, M., and Weisshaar, E. 1988. *Astr. Ap.* **194**, 257.

Harvey, J. W. 1977 in *Heighlights of Astronomy* 4, ed. E. A. Müller (Dordrecht: D. Reidel Publishing Co.), p. 223.

Hasan, S. S. 1985, *Astr. Ap.*, **143**, 39.

Hickey, J., Alton, B., Kyle, L., and Hoyt, D. 1988, *Space Sci. Rev.*, **48**, 321.

Hirayama, Tadashi, Hamana, Shigeo, and Mizugaki, Kakuo. 1985, *Solar Phys.* **99**, 43.

Howard, Robert F. 1991. *Solar Phys.*, **134**, 233.

Hudson, H.S. 1988, *Ann. Rev. Astr. Ap.*, **26**, 473.

Keil, S. L. 1977, *Solar Phys.*, **53**, 359.

Knölker, M., Schüssler, M., and Weisshaar, E. 1988. *Astr. Ap.* **194**, 257.

Knölker, M., and Schüssler, M. 1988, *Astr. Ap.*, **202**: 275.

Lawrence, John K. 1988, *Solar Phys.*, **116**, 17.

Lawrence, J. K., Chapman, G. A., and Herzog, A. D. 1988, *Ap. J.*, **324**, 1184.

Lawrence, J. K., Chapman, G.A., and Walton, S.R. 1991, *Ap. J.*, **375**, 771.

Livingston, W., Wallace, L., and White, O. 1988, *Science*, **240**, 1765.

Muller, R. 1983, *Solar Phys.*, **85**, 113.

Muller, R. and Keil, S. L. 1983. *Solar Phys.*, **87**, 243.

Muller, R. 1985, *Solar Phys.*, **100**, 237.

Oster, L. Schatten, K. H., and Sofia, S. 1982. *Ap. J.*, **256**, 768.

Scharmer, G. B. Brown, D. S., Pettersson, L., and Rehn, J. 1985. *Appl. Optics*, **24**, 2558.

Scharmer, G. B. 1989, in *Solar and Stellar Granulation*, eds. Robert J. Rutten and Guiseppe Severino, (Dordrecht: Kluwer Academic Publications), p. 161.

Scharmer, G. B. 1990, *private communication.*

Schüssler, M., and Solanki, S. K. 1988, *Astr. Ap.*, **192**, 338.

Spruit, H. C. 1976, *Solar Phys.*, **50**, 269.

Steiner, O., Pneuman, G. W., and Stenflo, J. O. 1986, *Astr. Ap.*, **170**, 126.

Stenflo, J. O. 1989, *Astron. Ap. Rev.*, **1**, 3.

Title, A. M., Tarbell, T. D., Topka, K. P., Ferguson, S. H., Shine, R. A., and the SOUP Team. 1989, *Ap. J.*, **336**, 475.

Title, T., Tarbell, T., Topka, K., Cauffman, D., Balke, C., and Scharmer, G. 1990, in *Physics of Magnetic Flux Ropes*, eds. C. T. Russel, E. R. Priest, and L. C. Lee, (Washington DC: American Geophysical Union), p. 171.

Title, Alan M., Topka, Kenneth P., Tarbell, Theodore D., Schmidt, Wolfgang, Balke, Christiaan, and Scharmer, Göran. 1991, *Ap. J.*, in press.

Topka, K. P., Tarball, T. D., and Title, A. M. 1986, *Ap. J.*, **306**, 304.

Zayer, I., Solanki, S. K., and Stenflo, J. O. 1989. *Astr. Ap.*, **211**, 463.

Zirin, H. 1988, *Astrophysics of the Sun* (Cambridge: Cambridge Univ. Press), p. 131.

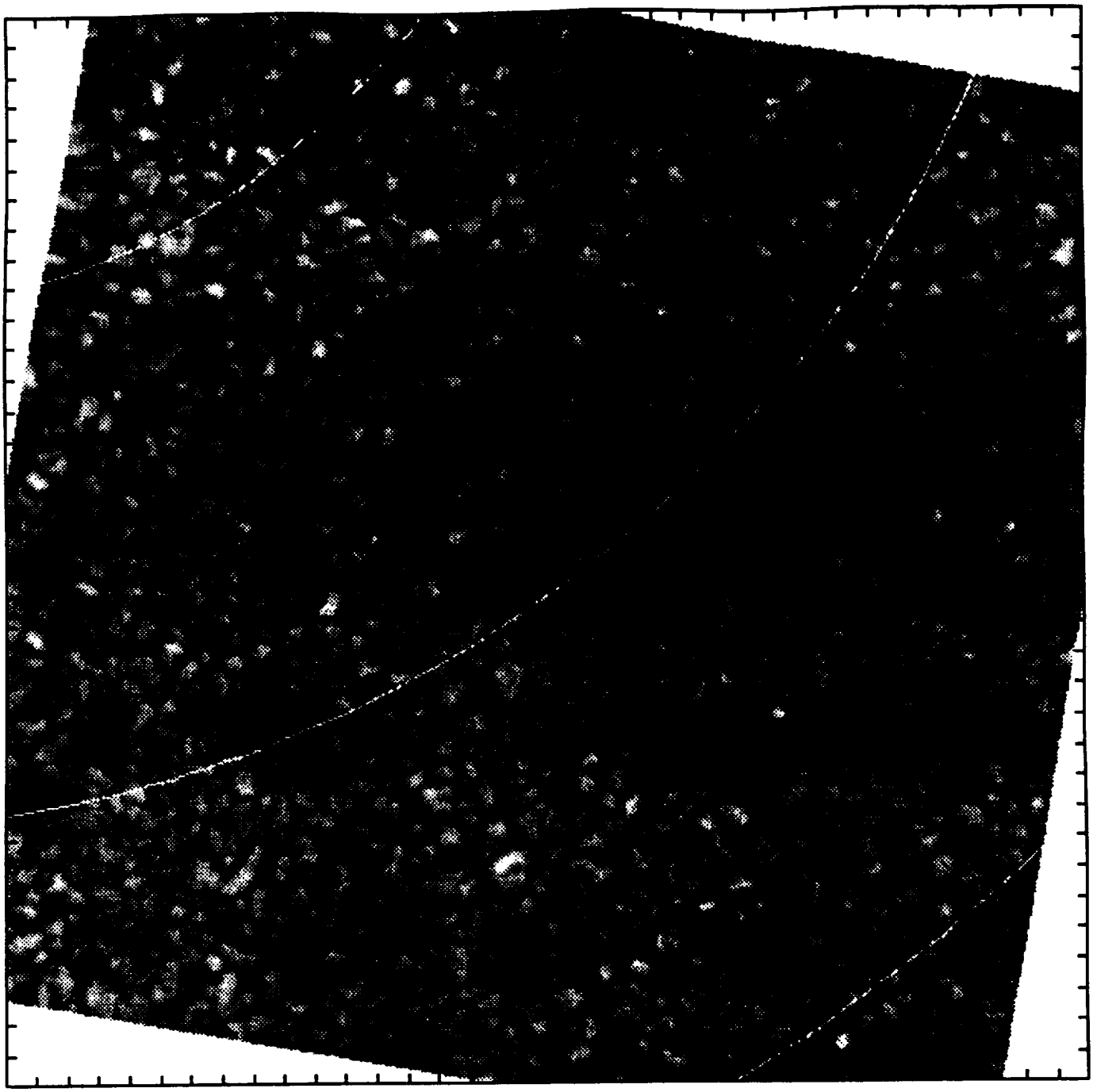

Figure 1a. Image of the continuum taken on June 6, 1990, at 08:25 UT. A $70'' \times 70''$ portion of AR 6085 is shown at 5576Å. The smallest features visible on the original are $0.3''$ across. North is at the top, east is on the left. The arcs represent heliocentric angles of 3°, 5°, and 7°. The tick marks are 2 arcseconds apart.

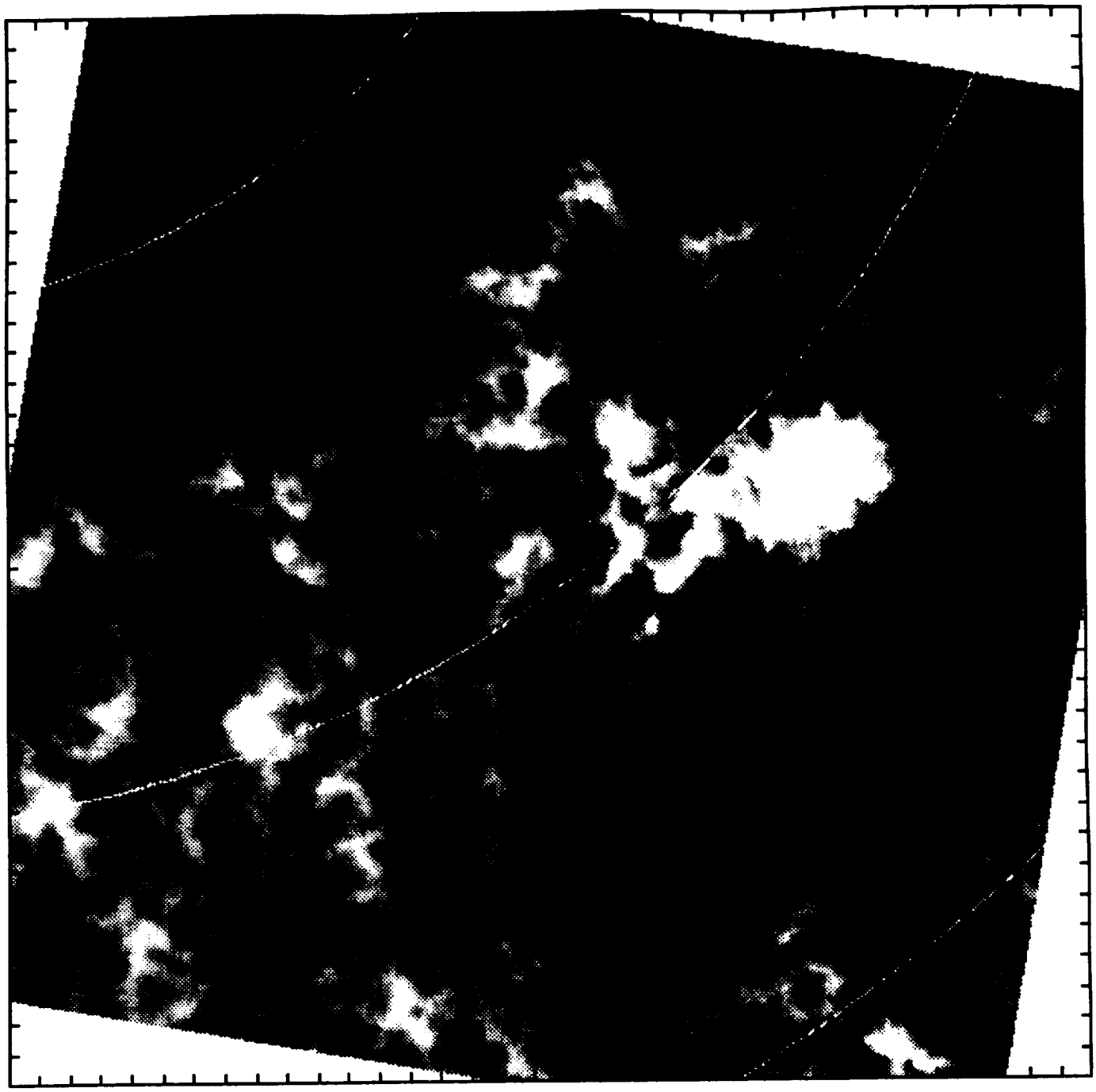

Figure 1b. Magnetogram taken on June 6, 1990. This image is the result of combining 8 individual filtergrams in Fe I 6302 Å, taken about 30 s before the continuum image of 1a. Both have been carefully registered.

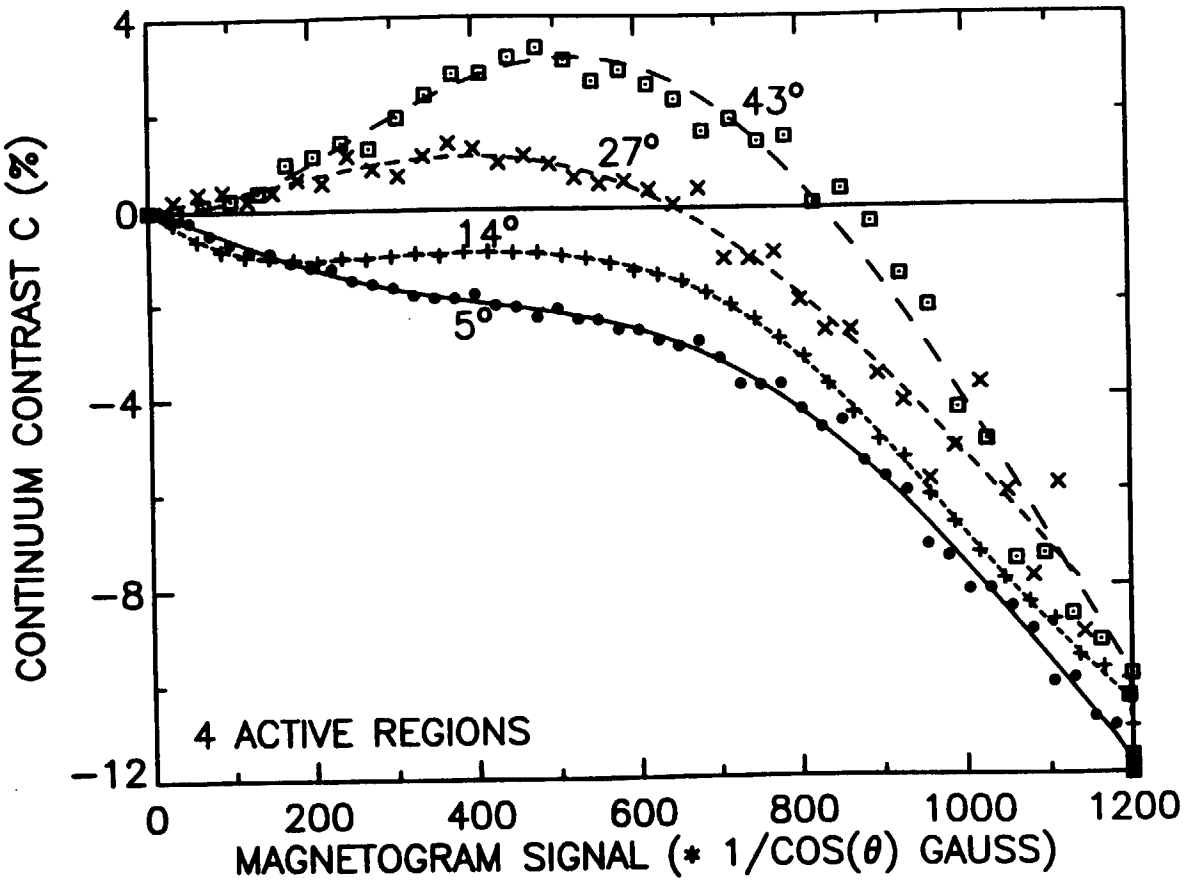

Figure 2. Mean continuum contrast C of faculae versus magnetogram signal for 4 active regions. Each measurement is labeled by its mean heliocentric distance θ. Note that for 5° and 14°, C is negative for all non-zero values of the magnetic signal. The magnetogram signal has been corrected for the line of sight by dividing by $cos(\theta)$.

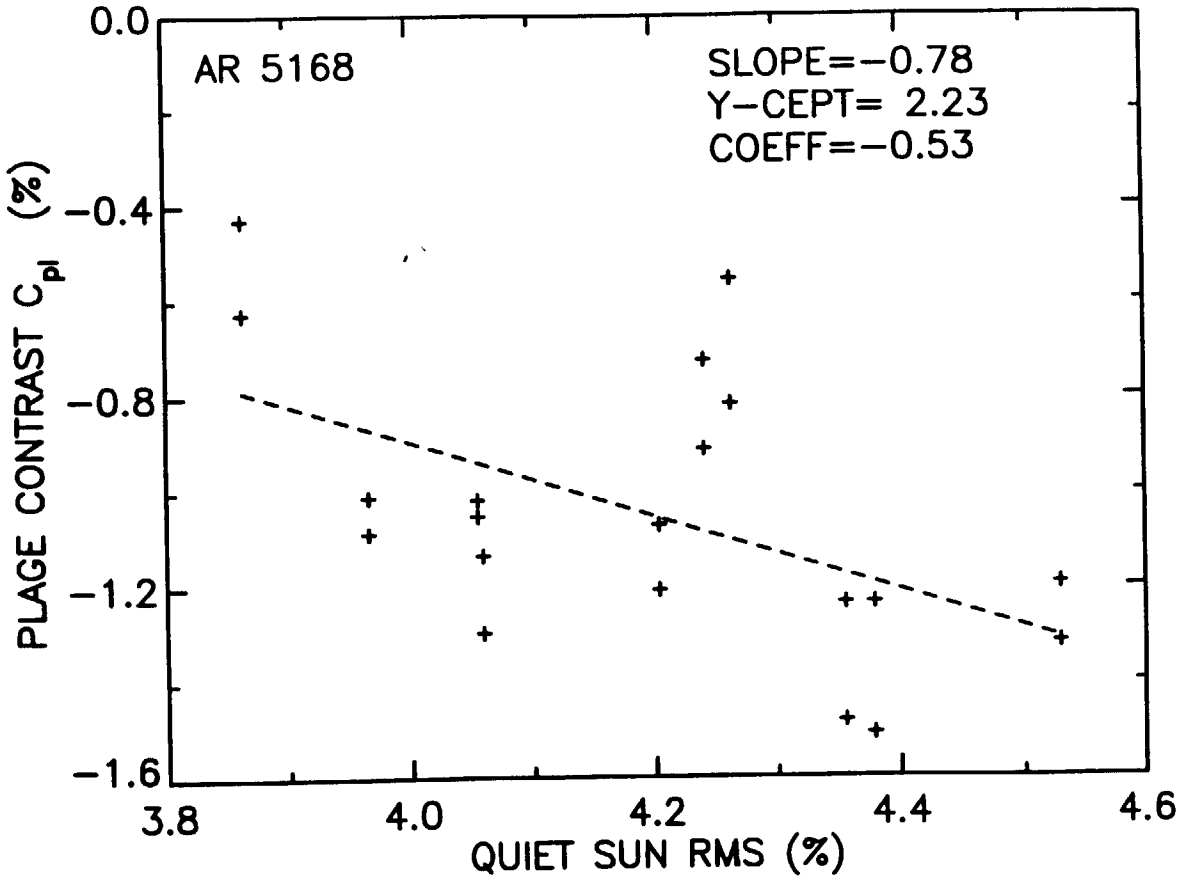

Figure 3. Scatter plot showing measured contrast in faculae, C_{pl}, versus rms contrast in the quiet sun, which is being used as a proxy for atmospheric seeing.

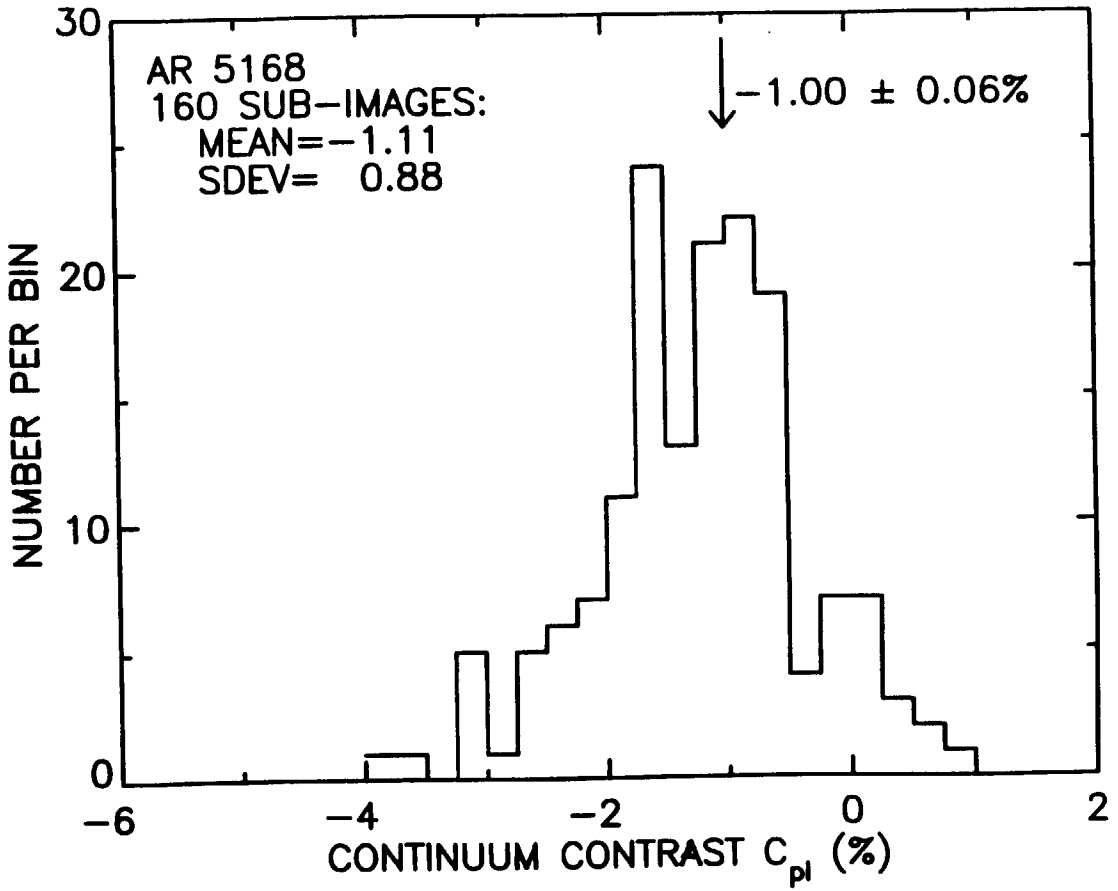

Figure 4. Histogram showing 160 independent measurements of facular contrast, C_{pl}, obtained by dividing 10 frames from the 1988 September 29 observation into 16 sub-images each. The mean of C_{pl} for the same 10 frames, traeting each frame as a single image, is shown by the vertical arrow at -1.00% for reference.

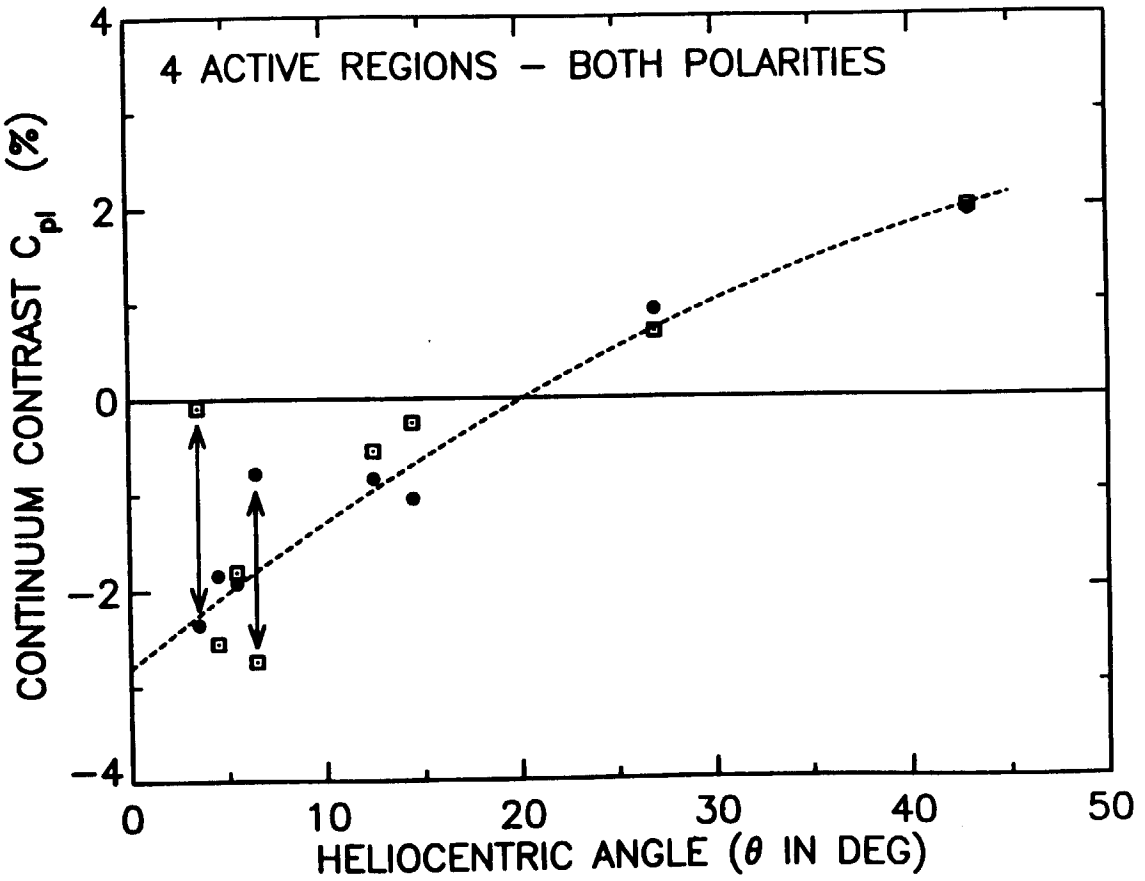

Figure 5. Variation in facular contrast, C_{pl}, with heliocentric angle for positive polarity (dots), and negative polarity (boxes). The arrows indicate where large differences in C_{pl} exists between positive and negative polarity, indicating large relative inclination.

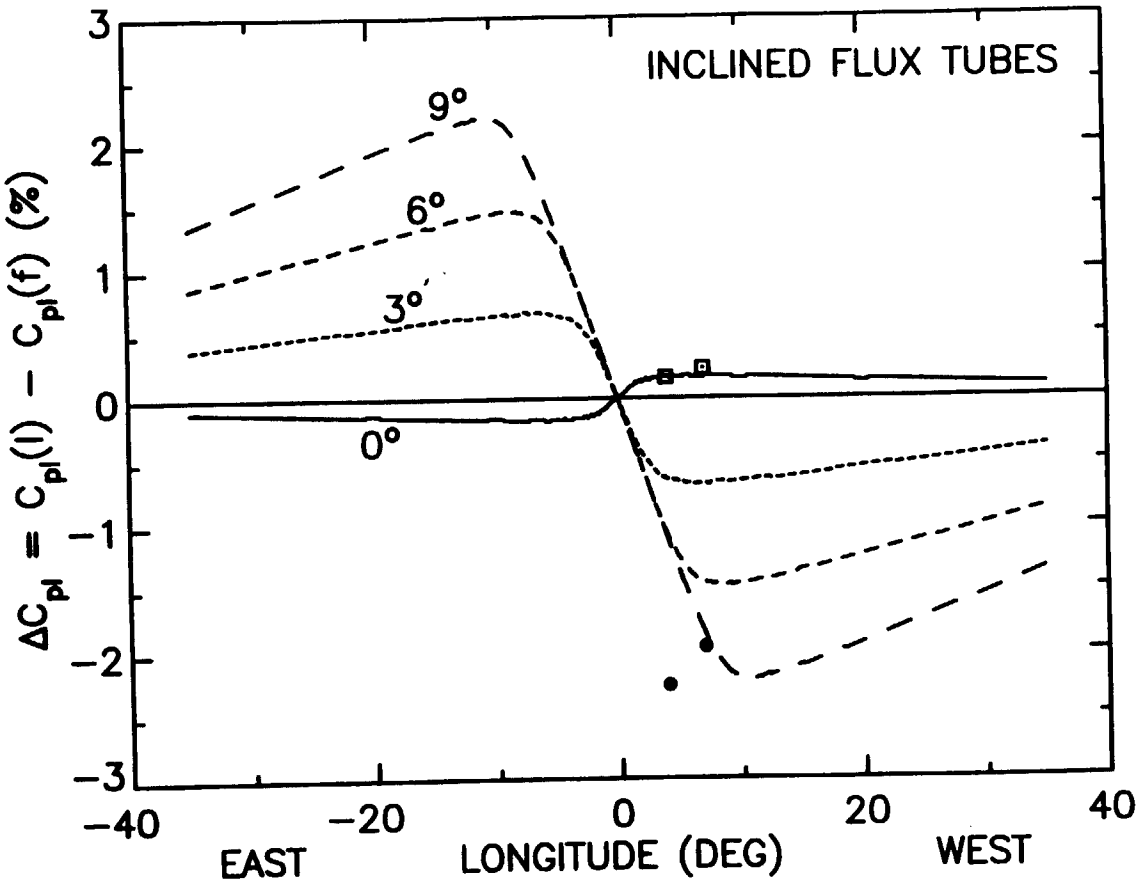

Figure 6. $\Delta C_{pl} = C_{pl}(l) - C_{pl}(f)$ as a function of longitude of the center of masss of a simple bipole 20″ in size. It is assumig to be oriented east-west. ΔC_{pl} is shown for inclinations from local vertical of 0°, 3°, 6°, and 9°. In this calculation both the leading and following polarities are assumed to be inclined toward each other by the same amount.

Figure 7. Magnetogram from the 1989 July 3 observation. The box in the lower right outlines region 2. The rest of the image is region 1. See text. The tick marks are 2 arcseconds.

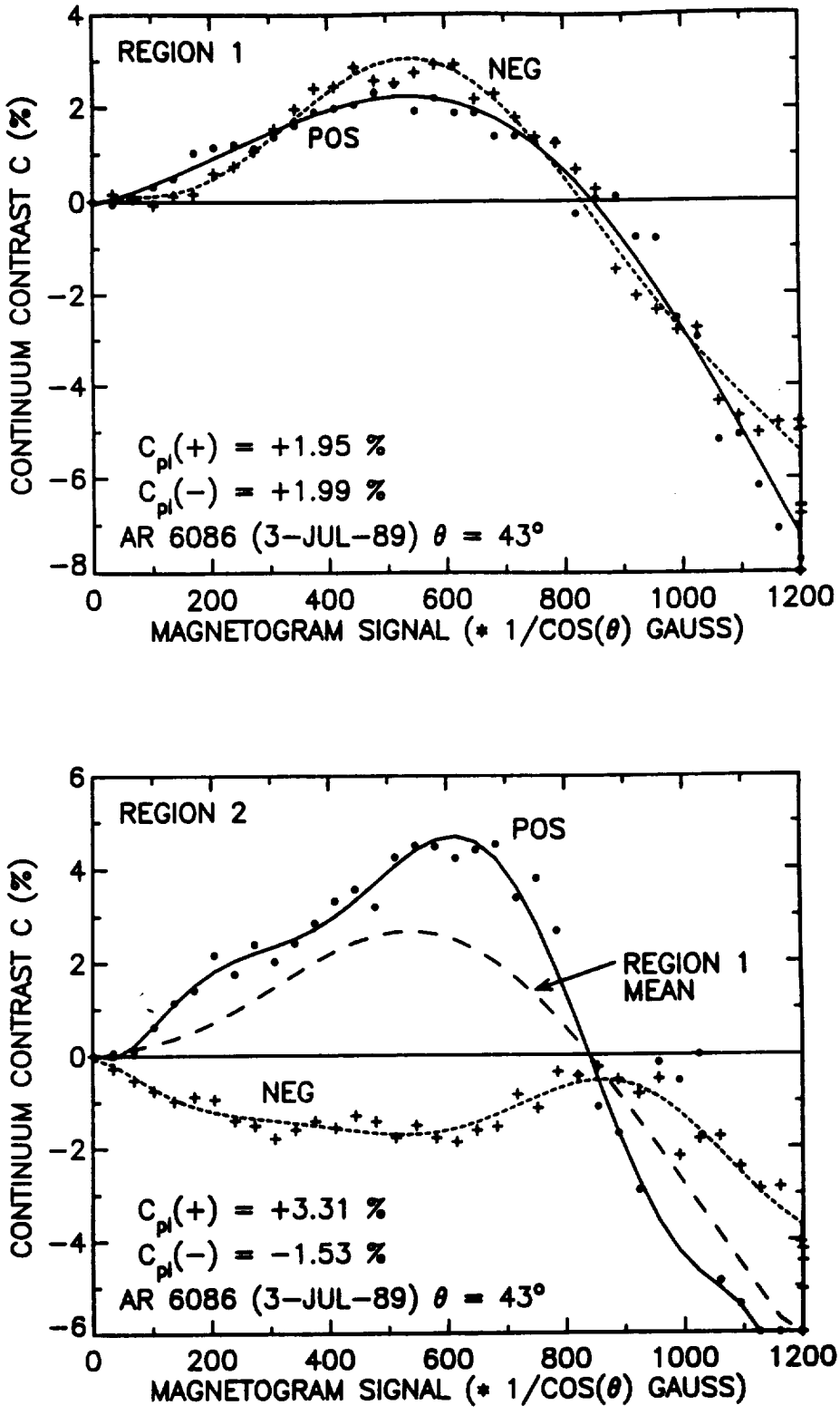

Figure 8. Facular contrast versus magnetogram signal for both polarities in region 1 (*a*), and region 2 (*b*) of the 1989 July 3 observation. Regions 1 and 2 are defined in the last figure. The small difference in (*a*) between polarities indicates little relative inclination, while and large difference in (*b*) indicates large relative inclination. The dashed curve between measurements in (*b*) is the average from (*a*).

NASA
National Aeronautics and Space Administration

Report Documentation Page

1. Report No.	2. Government Accession No.	3. Recipient's Catalog No.
P009805		

4. Title and Subtitle
INVESTIGATION OF SOLAR ACTIVE REGIONS AT HIGH RESOLUTION BY BALLOON FLIGHTS OF THE SOLAR OPTICAL UNIVERSAL POLARIMETER, Definition Phase.

5. Report Date

6. Performing Organization Code

7. Author(s)
Dr. Theodore D. Tarbell
Dr. Kenneth P. Topka

8. Performing Organization Report No.

10. Work Unit No.

9. Performing Organization Name and Address
Lockheed Missiles and Space Co., Inc.
Lockheed Palo Alto Research Laboratory
3251 Hanover St. Dept. 91-30, B/252
Palo Alto, CA 94304

11. Contract or Grant No.
NAS8-38106

13. Type of Report and Period Covered
FINAL
July 1989 to March 1992

12. Sponsoring Agency Name and Address
National Aeronautics and Space Administration
George C. Marshall Space Flight Center
Marshall Space Flight Center, AL 35812

14. Sponsoring Agency Code

15. Supplementary Notes

16. Abstract
This report describes the definition phase of a scientific study of active regions on the sun by balloon flight of a former Spacelab instrument, the SOLAR OPTICAL UNIVERSAL POLARIMETER (SOUP). SOUP is a optical telescope with image stabilization, tunable filter, and various cameras. After the flight phase of the program was cancelled due to budgetary problems, scientific and engineering studies relevant to future balloon experiments of this type were completed. High resolution observations of the sun were obtained using SOUP components at the Swedish Solar Observatory in the Canary Islands. These were analyzed and published in studies of solar magnetic fields and active regions. In addition, testing of low-voltage piezoelectric tranducers was performed, which showed they were appropriate for use in image stabilization on a balloon.

17. Key Words (Suggested by Author(s))	18. Distribution Statement
Balloon flight, piezoelectric transducers, solar physics, solar magnetic fields, solar faculae.	Unclassified-Unlimited

19. Security Classif. (of this report)	20. Security Classif. (of this page)	21. No. of pages	22. Price
Unclassified	Unclassified	45	NSP

NASA FORM 1626.OCT 86